

TECH LIBRARY KAFB, NM
0144502

1284

8033

NATIONAL ADVISORY COMMITTEE FOR AERONAUTICS

TECHNICAL NOTE

No. 1284

INVESTIGATION AT LOW SPEED OF THE LONGITUDINAL
STABILITY CHARACTERISTICS OF A 60° SWEPT-BACK
TAPERED LOW-DRAG WING

By John G. Lowry and Leslie E. Schneiter
Langley Memorial Aeronautical Laboratory
Langley Field, Va.

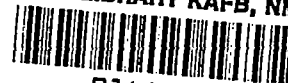


Washington

May 1947

**AFMDC
TECHNICAL LIBRARY
AFL 2811**

319.98/41



NATIONAL ADVISORY COMMITTEE FOR AERONAUTICS

TECHNICAL NOTE NO. 1284

INVESTIGATION AT LOW SPEED OF THE LONGITUDINAL
STABILITY CHARACTERISTICS OF A 60° SWEEP-BACK
TAPERED LOW-DRAG WING

By John G. Lowry and Leslie E. Schreiber

SUMMARY

An investigation was made in the Langley 300 MPH 7- by 10-foot tunnel to determine at low speed the longitudinal stability characteristics of a 60° swept-back, tapered, low-drag wing of aspect ratio 2.55. Several modifications were made to this wing in an attempt to improve its longitudinal stability characteristics.

The results show undesirably large changes in the longitudinal stability characteristics of the 60° swept-back wing. The most effective modification consisted in an alteration to the plan form of the wing by extending the leading edge forward about half a chord length over the outer 25 percent of the span. The maximum lift coefficient of the swept-back wing was about the same as that of the unswept wing, but the angle of attack for maximum lift of the swept wing was more than twice that of the straight wing. Decreasing the aspect ratio from 2.55 to 1 improved the longitudinal stability characteristics of the wing, particularly in the range of high lift coefficient.

The results of testing the wing with a deflectable tip showed little promise with regard to improvement of the longitudinal stability characteristics, but deflecting the tip offered interesting possibilities as a means of longitudinal and lateral control.

INTRODUCTION

The problem of producing airplanes capable of flight speeds equal to and greater than the speed of sound with a reasonable expenditure of power has been studied by airplane designers for some time. In order to solve this problem it is necessary to design an airplane that does not exhibit a sharp drag rise near the speed of sound. Reference 1 proposes the use of highly swept wings as one

method of eliminating this sharp drag rise. The analysis of reference 1 is based on the assumption that only the component of the free-stream flow normal to the wing leading edge affects the pressure distribution over the wing, and thus the critical flight Mach number will be increased by the ratio of one over the cosine of the angle of sweep. This analysis also indicates that the flow affecting the forces and moments of the wing is subsonic so long as the wing remains inside the Mach cone. Much information on the stability and control of a swept wing to be used at high speeds can therefore be obtained at relatively low speeds.

Much work has been done on wings having angles of sweepback up to 45° but information on wings having sweepback greater than 45° is meager. In order to obtain a better understanding of the problems involved with angles of sweep greater than 45° , tests of an exploratory nature were performed on a 60° swept-back, tapered, low-drag wing. One of the problems was to improve the longitudinal stability characteristics indicated in reference 2 for a 60° swept-back wing. Wing-plan-form variations, leading-edge slats (both full and partial span), and a partial-span leading-edge flap were investigated in an attempt to improve the longitudinal characteristics of the wing. Tests of several trailing-edge flaps were made to supplement the results of reference 2.

APPARATUS AND MODELS

A semispan swept-back-wing model was mounted in the Langley 300 MPH 7- by 10-foot tunnel as shown in figure 1. The root chord of the model was adjacent to the ceiling of the tunnel, the ceiling thereby serving as a reflection plane. Although only a very small clearance was maintained between the root chord and the tunnel wall, no part of the model was fastened to or in contact with the tunnel wall. The model was so arranged on the balance frame that all forces and moments acting on it might be determined. A semicircular root fairing was attached to the model to deflect the air flowing into the test section through the clearance hole around the attachment strut in order to minimize its effect on the flow over the model.

The model used for these tests was constructed of mahogany to the plan form indicated in figure 2. The airfoil section normal to the quarter-chord line was constant throughout the span and was of NACA 65-210 airfoil profile. The plain wing or the wing with any of the plan-form variations had a semicircular faired tip. Wing-plan-form variations involving a change in aspect ratio were made by cutting off the wing at the stations indicated in figure 3 and adding a semicircular faired tip.

The leading- and trailing-edge extensions shown in figures 4, 5, and 6 were made of thin plywood and had flat surfaces that faired smoothly into the contour of the wing. The partial-span slats and leading-edge flap shown on figures 7, 8, and 9 were of Navy N-22 airfoil section and were supported on the wing by three $\frac{1}{4}$ -inch-thick aluminum brackets. The full-span slat (shown in fig. 10) was made of thin aluminum sheet formed to the contour of the leading edge of the wing and was supported by six $\frac{3}{8}$ -inch wooden brackets. The trailing-edge flaps, shown in figure 11, were made of $\frac{1}{4}$ -inch plywood and were attached to the wing with steel fittings.

The wing with the raked tip and the deflectable tip is shown in figure 12. The deflectable tip, both sealed and slotted (see fig. 12), was attached to the model by steel straps. The slotted tip was supported by straps on the lower surface only, and a sheet-aluminum lip was added to the upper surface to give the desired slot gap.

The leading-edge deflector plates shown in figure 13 were made of soft metal strips bent to the contour of the leading edge of the wing and attached with wire brads.

SYMBOLS

C_D	drag coefficient (D/qS)
C_L	lift coefficient (L/qS)
$C_{m_{a.c.}}$	pitching-moment coefficient ($M/qS\bar{c}$) about aerodynamic center
D	drag, pounds
L	lift, pounds
M	pitching moment, foot-pounds
q	dynamic pressure, pounds per square foot ($\rho v^2/2$)
S	area of the semispan wing, square feet

- \bar{c} mean aerodynamic chord, feet
- c local chord
- A aspect ratio $(b^2/2S)$
- Λ sweep angle (quarter-chord line), degrees
- α angle of attack measured in reflection plane, degrees
- ρ mass density of air, slug per cubic foot
- V free-stream air velocity, feet per second
- b twice the span of the model, feet
- C_{L_α} slope of the curve of lift coefficient against angle of attack, measured at zero lift
- η aspect-ratio correction factor, $\frac{\left(\frac{A_e}{A_e E_e + 2}\right)}{\left(\frac{A}{AE + 2}\right)}_{\Lambda = 0}$ (reference 2)
- A_e effective aspect ratio, aspect ratio of the swept wing divided by $\cos^2 \Lambda$
- E edge-velocity correction factor for lift of wing of aspect ratio A (reference 3)
- E_e edge-velocity correction factor for lift of wing of aspect ratio A_e , (reference 3).

CORRECTIONS

The force and moment coefficients for all but the reduced-aspect-ratio wings were determined with reference to the area and mean aerodynamic center of the plain wing. The coefficients for the reduced-aspect-ratio wings are based on the respective geometric characteristics of the wing.

The pitching-moment curves for all but the reduced-aspect-ratio wings are referred to the aerodynamic center of the plain wing as determined from the pitching-moment curve of the plain wing near zero lift. The pitching moments for the reduced-aspect-ratio wings are presented about their own aerodynamic centers as determined by the same method.

Since no jet-boundary corrections for swept wings were available and an investigation of such corrections is beyond the scope of this paper, corrections similar to those for unswept reflection-plane models were applied to the drag and angle of attack. The corrections applied were

$$\Delta C_{D_i} = \delta_w \frac{S}{C} C_{L_u}^2 = 0.0151 C_{L_u}^2$$

$$\Delta \alpha = \delta_w \frac{S}{C} C_{L_u} 57.3 = 0.866 C_{L_u}$$

where

- ΔC_{D_i} induced drag increment
- $\Delta \alpha$ increment of angle of attack
- δ_w boundary-correction factor (0.116 obtained from reference 4)
- S semispan wing area, square feet
- C tunnel-throat cross-sectional area (70 square feet)
- C_{L_u} uncorrected lift coefficient

The data at angles of attack greater than 30° may be slightly in error since, at high angles of attack, the tip of the wing was close to the tunnel wall and no additional tunnel-wall corrections were applied.

No corrections were applied to the pitching-moment data. The data presented include the aerodynamic forces on the root fairing.

TESTS

Most of the tests were run at a dynamic pressure of 20.1 pounds per square foot, which corresponds to a Mach number of about 0.12 and a Reynolds number of about 2,370,000 based on the mean aerodynamic chord of the plain wing. For structural reasons, the trailing-edge-flap tests were run at a dynamic pressure of 10.1 pounds per square foot which corresponds to a Reynolds number of about 1,600,000.

The force tests, in general, were run through a range of angle of attack from -6° to 28° by 2° increments, except for that part of the range between 4° and 12° where the increment was decreased to 1° . The smaller increments were used so that the irregular part of the pitching-moment curve could be more accurately faired.

The trailing-edge-flap tests were made with the flap deflected 60° relative to the lower surface of the wing. The flap angle was measured in a plane mutually perpendicular to the quarter-chord line and the chord plane of the wing. For tests of deflectable wing tips either sealed or slotted, the tip was deflected relative to the chord plane. Tuft studies on the upper surface of the wing were made for most of the model configurations.

RESULTS AND DISCUSSION

The results of the force tests are presented in figures 14 to 26. Some of the tuft data are presented in figures 27 to 30. A list of the figures which show the results of the tests are presented in table I.

Plain wing.- Aerodynamic characteristics in pitch of the plain 60° swept-back wing (fig. 14) indicate that at a lift coefficient of about 0.2, an increase in stability amounting to a rearward shift in neutral point of about 14.4 percent of the mean aerodynamic chord occurs. This stable moment variation extends up to a lift coefficient of 0.5 at which point the moment begins to become violently unstable. In the range of low lift coefficient, the lift-curve slope $C_{L\alpha}$ is very nearly linear but shows an increase at a lift coefficient of about 0.2. This increase in slope corresponds to the stable shift of the pitching-moment curve and indicates that the increase in lift is occurring at, or near, the tip of the wing.

The stabilizing moment that occurs between lift coefficients of 0.2 and 0.5 may be associated with the roughness of the flow over the leading edge of the wing as shown on the tuft pictures (fig. 27) as well as with the increase in lift over the tip portion of the wing. This roughness or separation existing over the first few percent of the airfoil chord can very probably be explained to some extent if it is remembered that there is a cross flow along the wing span which builds up boundary layer. This theory is substantiated by the examination of the tuft pictures for the wing with leading-edge deflector plates (fig. 23) which show that the plates retard the cross flow along the leading edge, with the result that the roughness and stabilizing moment do not occur. (See fig. 17.)

When the slope of the pitching-moment curve becomes unstable, the lift curve shows a decided decrease in slope. A correlation of the tuft pictures (fig. 27) and pitching-moment curve indicate that as the pitching-moment curve becomes increasingly less stable and finally, at a lift coefficient of about 0.5, becomes unstable, the boundary layer on the wing is tending to flow more nearly parallel to the quarter-chord line. Visual analysis of the flow over the wing, made by using tufts placed on staffs about five inches high, showed that at angles of attack between 12° and 16° , a layer of air 5 or more inches thick covering the entire chord is flowing approximately parallel to the quarter-chord line over the outer portion of the wing. This body of air very probably causes the loss in lift at the wing tip, which accounts for the unstable moment on the wing. No distinct separation, however, could be detected by surface tufts in this region.

The maximum lift coefficient of the 60° swept-back wing is about the same as that previously obtained (unpublished data) on a complete wing having 0° sweep of the quarter-chord line from which the panel used for these tests was obtained. The angle of attack for maximum lift is about 33° for the swept wing as compared with 15° for the unswept wing.

Revisions to plain wing. - In an attempt to improve the unsatisfactory characteristics of the plain wing, numerous revisions to the model were tested. These revisions were designed not so much to determine their practicality but mainly to determine the type of device that would be required. The determination of whether the devices would have to be retracted for the high-speed condition was beyond the scope of this investigation. Figures 15 to 21 show the effects of these various revisions to the model. The simplest conclusion reached from a study of the data is that almost any revision to the leading edge of the wing will tend to eliminate the stabilizing moment obtained at a low lift coefficient with the plain wing but may have little effect upon the destabilizing moment which occurs at a

slightly higher lift coefficient. Of the revisions to the model that prevented the stabilizing moment at low lift, the simplest was the raked tip (fig. 18). The raked tip did not, however, eliminate the unstable moment break at a lift coefficient of about 0.5. The most effective revision to the model, with reference to the elimination of any large changes in moment over a lift-coefficient range from 0 to 1.0, was the leading-edge extension I. (See figs. 4 and 15.) As is shown on figure 15, a lift coefficient of 1.0 was reached with a forward shift of the neutral point of 5.6 percent of the mean aerodynamic chord. This shift occurred at a lift coefficient of 0.5. This small change, as compared with the other revisions, may be attributed to the maintenance of an approximately linear lift curve at high angles of attack. Tuft studies (fig. 28) made of this and the other leading-edge extensions (fig. 5) show that the effect of the extension was such as to decrease to some extent the outflow along the wing and thus to assist the tip in maintaining lift. The addition of the trailing-edge extension (fig. 6) to the wing with the leading-edge extension also gave a satisfactory variation of pitching moment throughout the lift-coefficient range up to 1.0. (See fig. 16.) Tuft photographs of the wing with the partial-span slats and leading-edge flap are shown in figure 28.

Reduced-aspect-ratio wings.- The results with the reduced-aspect-ratio wings (fig. 22) indicate that as the aspect ratio decreases, the unstable portion of the pitching-moment-coefficient curve tends to become more stable, becoming about neutrally stable at $A = 1.50$ and stable at $A = 1.00$. As would be expected, the slope of the lift curve decreases, and the drag for a given lift increases as the aspect ratio decreases. Figure 22 also shows that the lift-curve slope, as determined from these data, decreases more rapidly with decreasing aspect ratio than is indicated by the theoretical considerations given in reference 2. The lift-curve slope for the wing of aspect ratio 2.55, however, checks very well with both the theoretical and the experimental lift-curve slope presented in reference 2.

A study of the tuft pictures taken of the reduced-aspect-ratio wings (fig. 30) shows that the air flow at a given spanwise location for each aspect ratio at the same angle of attack is very nearly the same. This similarity indicates that, if the spanwise flow shown on the wing of aspect ratio 2.55 is the cause of the loss of lift at the tip and the consequent unstable moment, removal of that part of the wing where the spanwise flow occurs will eliminate the unstable moment. This hypothesis is borne out by the fact that as the aspect ratio decreased (tip removed), the magnitude of the unstable moment decreased, and the moment finally became stable.

Deflectable tips.- The results of the tests with the deflectable tips (fig. 12) are shown in figures 23 and 24. It may be seen that there was no improvement in the pitch characteristics of the wing with droop or dihedral in the tip. These results are in agreement with those of reference 2. The deflectable tip, either slotted or sealed, however, appears to be an interesting possibility as a means of both lateral and longitudinal control. Calculations made on the basis of these data and some unpublished data indicate that good rates of roll may result from 20° deflection of the tip. No data are available to indicate the magnitude of the hinge moments on a control surface of this type, but it is felt that a reasonably well balanced surface could be devised.

Flap conditions.- The effectiveness of a 0.20c split-type flap deflected 60° and placed at the 0.80, 0.90, and 1.00c lines is shown in figure 25. As would be expected from data on wings without sweep, the 0.50-span flap located on the trailing edge (1.00c) produced the largest increment of lift of the three 0.50-span flaps tested. This flap gave a lift increment slightly larger than the full-span flap located on the 0.90-chord line.

The lift increment from a 0.50-span split flap (0.80c line) at 0° angle of attack was estimated from unswept wing data from reference 2 by the methods given therein. The estimated lift-coefficient increment was 0.14. The increment obtained from these tests was 0.13. The effect of the flaps, as compared with the plain wing, was such as to produce a negative increment of pitching moment at a given lift coefficient. Figure 26 shows the effectiveness of the 0.50-span trailing-edge flap in providing a lift increment on the wing with the leading-edge extension 1. The lift increments are about equal on the wing with and without the leading-edge extension. The negative pitching-moment increment produced by the flap on the wing with the leading-edge extension was slightly larger than that produced by the same flap on the plain wing.

CONCLUSIONS

The results of tests at low speed of a low-aspect-ratio, tapered, highly swept-back, low-drag wing indicate that for the configurations tested:

1. For the plain wing at a lift coefficient of 0.2 an increase in stability amounting to a rearward shift in neutral point of about 14.4 percent of the mean aerodynamic chord occurred. At a lift coefficient of 0.5, the stability decreased and the wing became violently unstable.

2. The maximum lift coefficient of the swept wing was about the same as that of a wing formed by rotating the wing panel so that the quarter-chord line had 0° sweep, but the angle of attack for maximum lift was more than twice the value for the straight wing.

3. The longitudinal stability of the swept wing was best improved by the addition of an extension at the leading edge.

4. Wings of aspect ratios of about 1 or 1.5 had better longitudinal stability characteristics than wings of somewhat higher aspect ratios.

5. A drooped or dihedral tip had little effect in decreasing the large longitudinal stability changes with angle of attack but, however, showed possibilities as a means of effective longitudinal and lateral control.

Langley Memorial Aeronautical Laboratory
National Advisory Committee for Aeronautics
Langley Field, Va., August 5, 1946

REFERENCES

1. Jones, Robert T.: Wing Plan Forms for High-Speed Flight. NACA TN No. 1033, 1946.
2. Letko, William, and Goodman, Alex: Preliminary Wind-Tunnel Investigation at Low Speed of Stability and Control Characteristics of Swept-Back Wings. NACA TN No. 1046, 1946.
3. Swanson, Robert S., and Priddy, E. LaVerne: Lifting-Surface-Theory Values of the Damping in Roll and of the Parameter Used in Estimating Aileron Stick Forces. NACA ARR No. L5F23, 1945.
4. Silverstein, Abe, and White, James A.: Wind-Tunnel Interference with Particular Reference to Off-Center Positions of the Wing and to the Downwash at the Tail. NACA Rep. No. 547, 1935.

TABLE I.- FIGURES PRESENTING RESULTS
FOR VARIOUS CONFIGURATIONS OF 60° SWEEP-BACK WING

Figure	Configuration	Dynamic pressure, q (lb/sq ft)
Aerodynamic characteristics		
14	Plain wing	20.1
15	With leading-edge extension	20.1
16	Several combinations of leading-edge and trailing-edge extensions and slat 1	20.1
17	With six leading-edge deflector plates	20.1
18	With original and raked tip	20.1
19	With partial-span slat	20.1
20	With leading-edge flap	20.1
21	With full-span slat	20.1
22	With aspect ratio and taper ratio varied	20.1
23	With deflectable tip, slot sealed	20.1
24	With deflectable tip, slot open	20.1
25	With various 0.20c split flaps	10.1
26	{ With extension 1	20.1
	{ With extension 1 and $0.50\frac{b}{2}$, 0.20c flap	10.1
Tuft studies		
27	Plain wing	20.1
28	With leading-edge extension and six deflector plates	20.1
29	{ Plain wing	20.1
	{ With slat 1 or slat 2	20.1
	{ With leading-edge flap	20.1
30	With aspect ratio varied	20.1

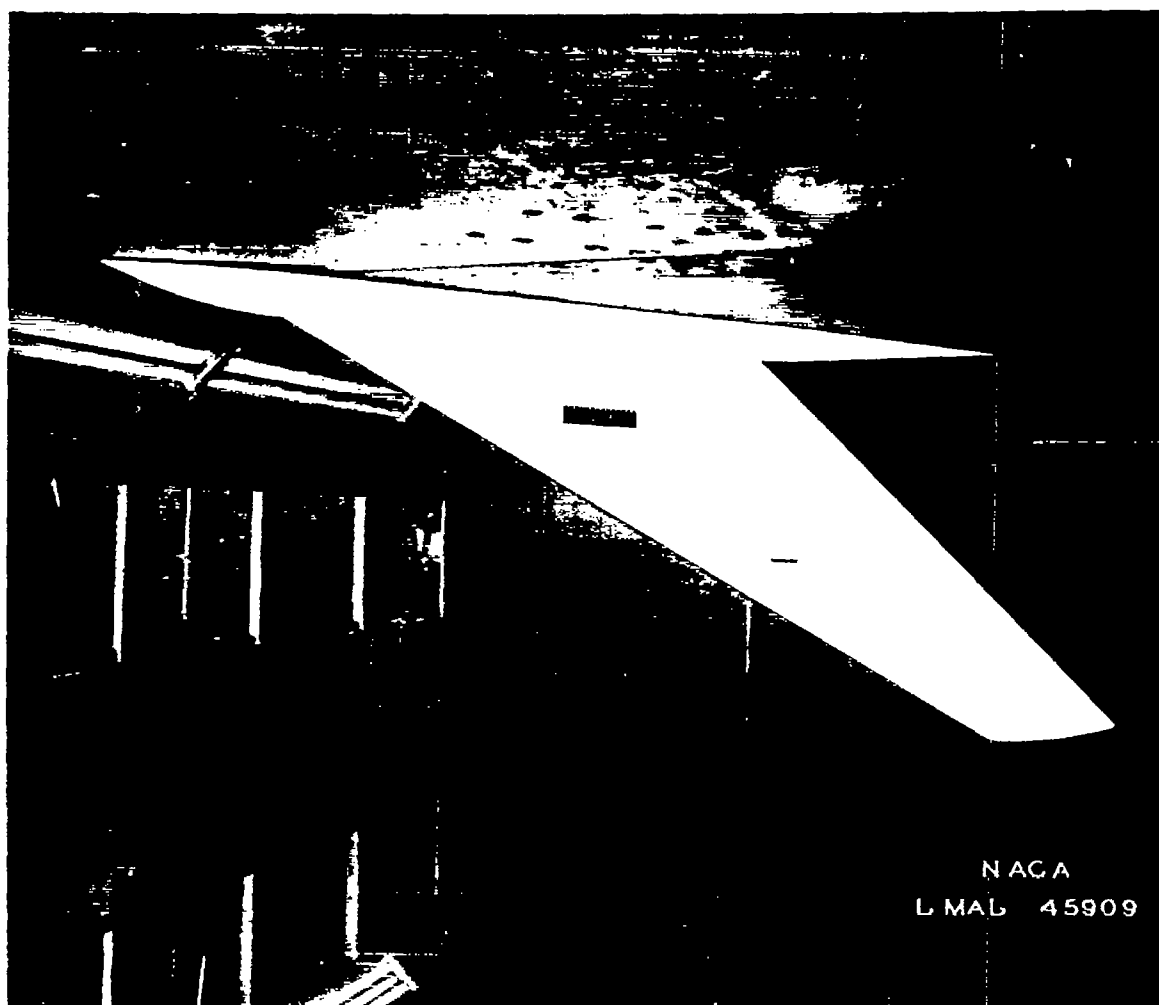
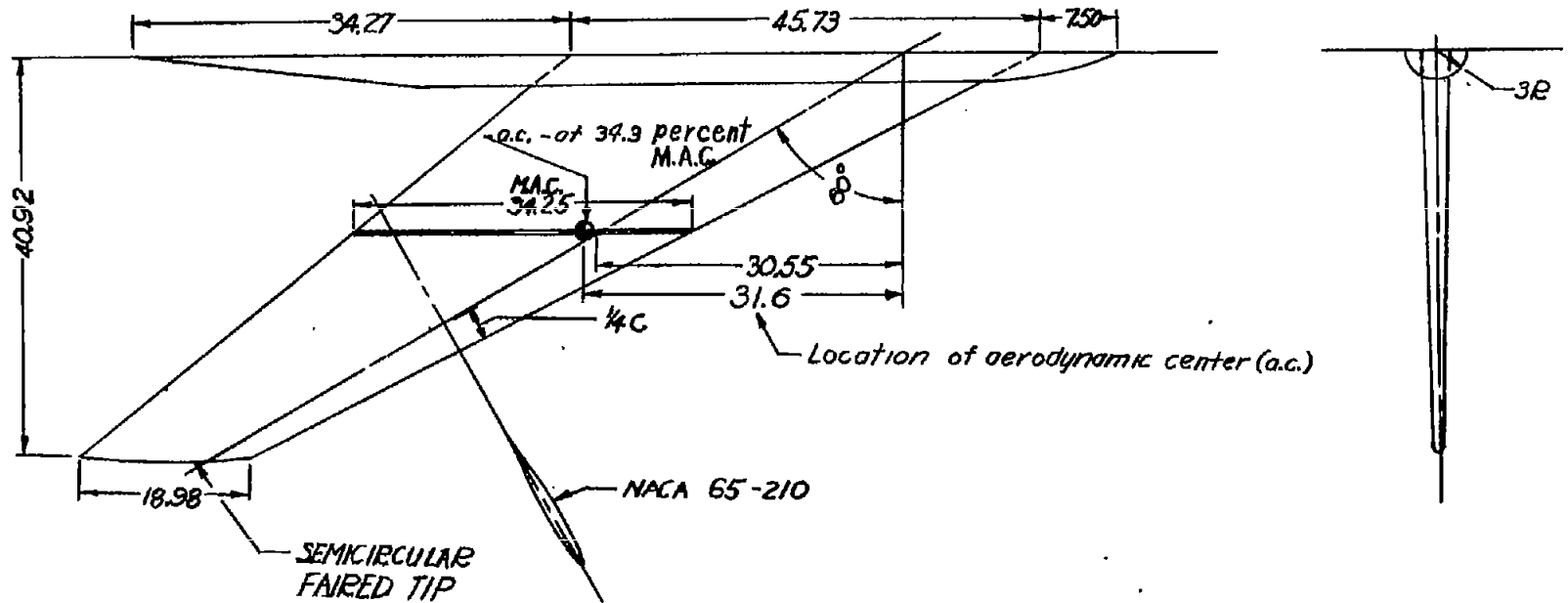
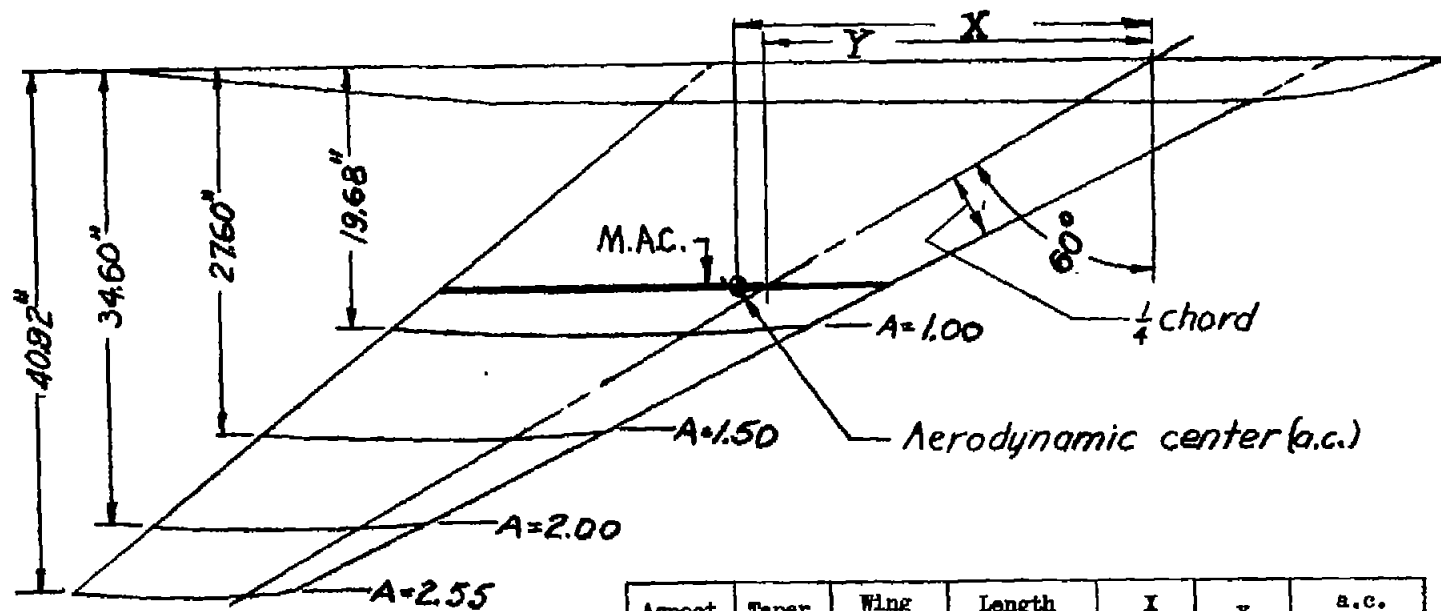


Figure 1.- The 60° swept-back wing as mounted in the Langley 300 MPH
7- by 10-foot tunnel.



NATIONAL ADVISORY
COMMITTEE FOR AERONAUTICS

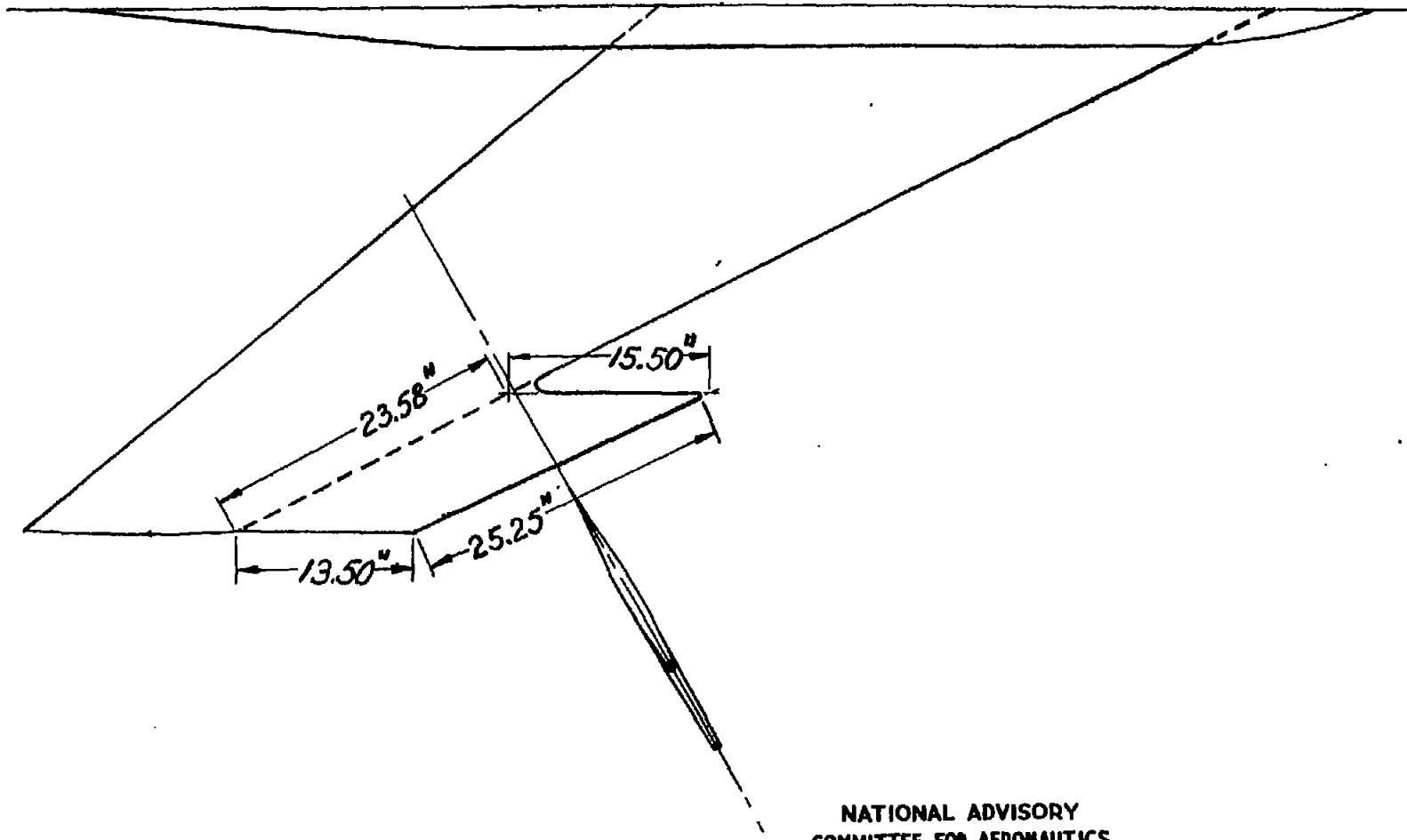
Figure 2.- Drawing of the 60° swept-back wing. $S = 9.12$ square feet; $A = 2.55$; taper ratio = 2.41.
(All dimensions in inches unless otherwise indicated.)



Aspect ratio	Taper ratio	Wing area (sq ft)	Length of M.A.C. (in.)	X (in.)	Y (in.)	a.c. (percent M.A.C.)
1.00	1.39	5.36	39.60	13.7	15.2	27.4
1.50	1.65	7.03	37.45	20.8	22.0	28.0
2.00	2.03	8.27	35.75	26.9	29.1	25.0
2.55	2.41	9.12	34.25	31.6	30.6	34.3

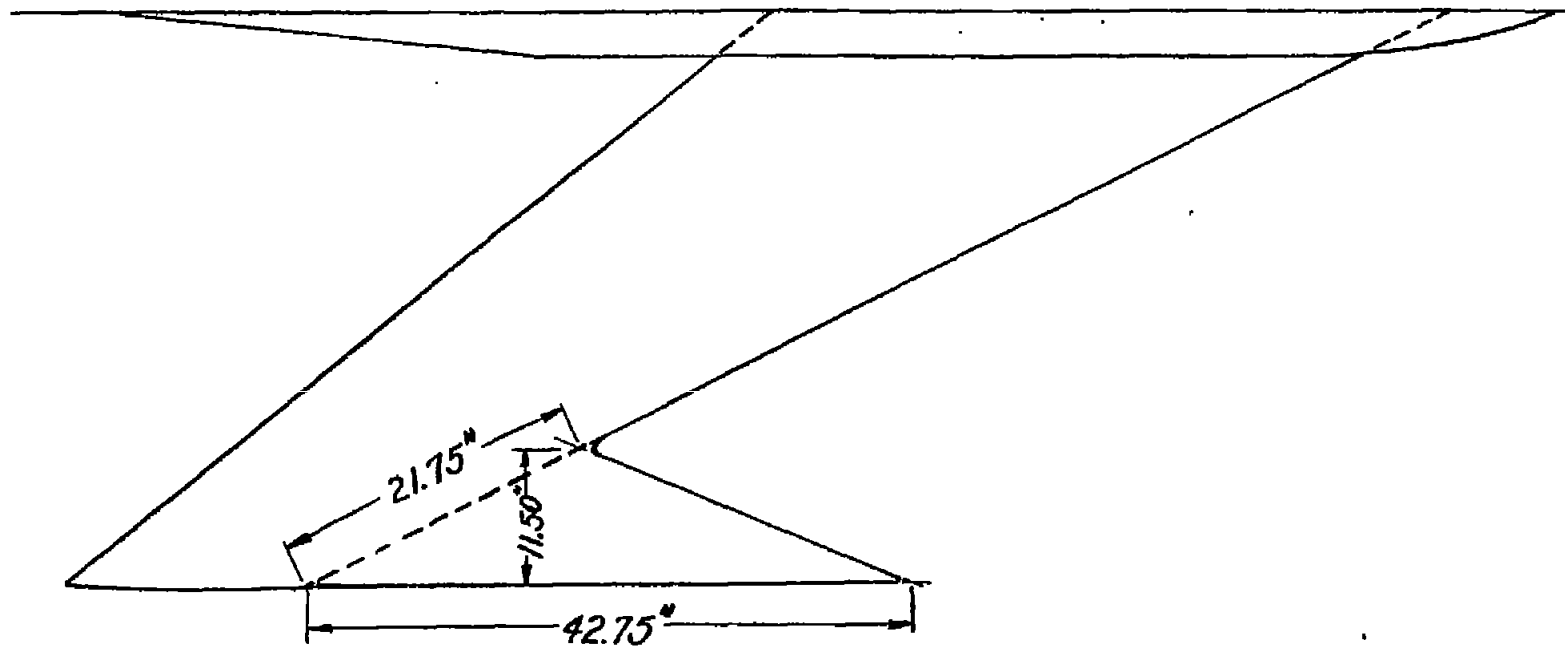
Figure 3.- Drawing of the 60° swept-back wings showing physical characteristics of various-aspect-ratio wings.

NATIONAL ADVISORY
COMMITTEE FOR AERONAUTICS



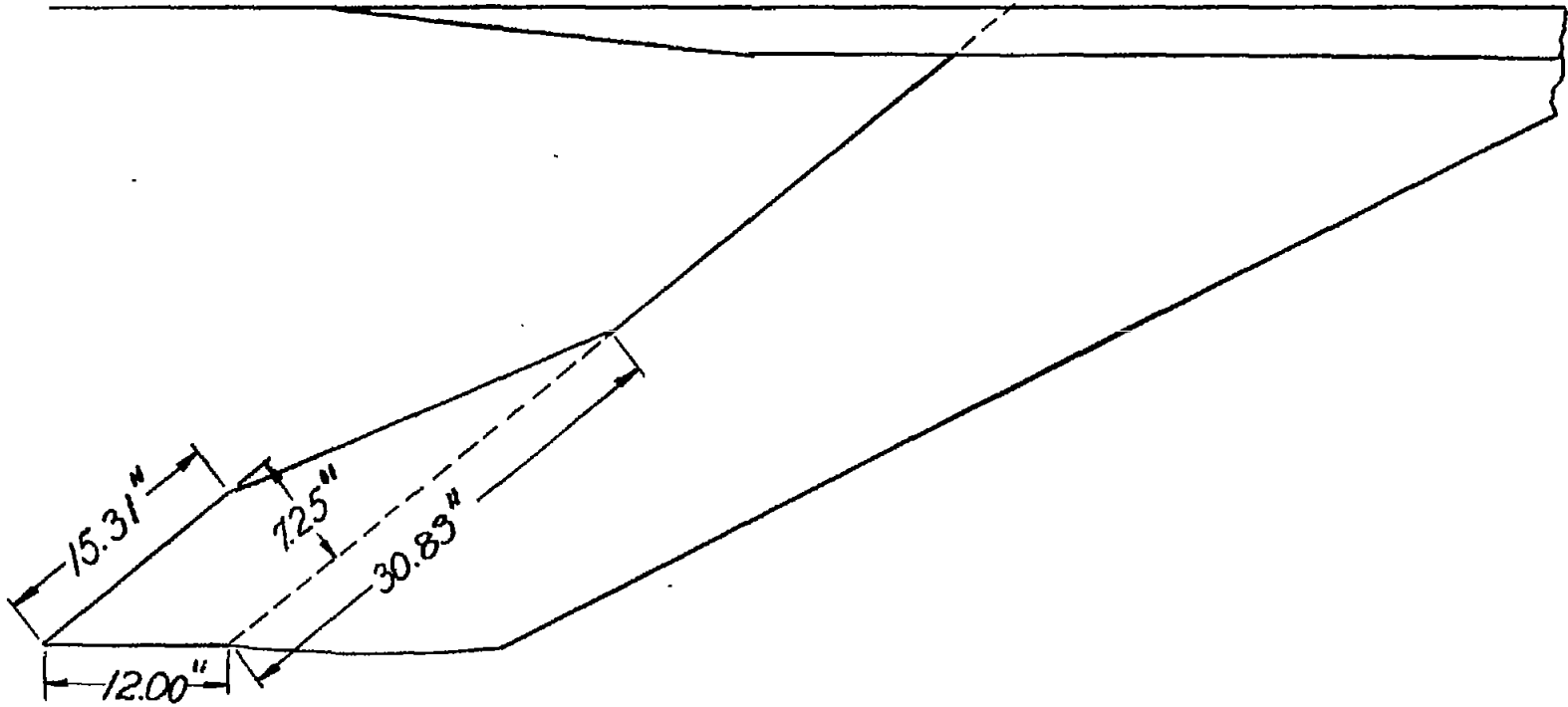
NATIONAL ADVISORY
COMMITTEE FOR AERONAUTICS

Figure 4.- Leading-edge extension 1. Area of extension,
1.13 square feet.



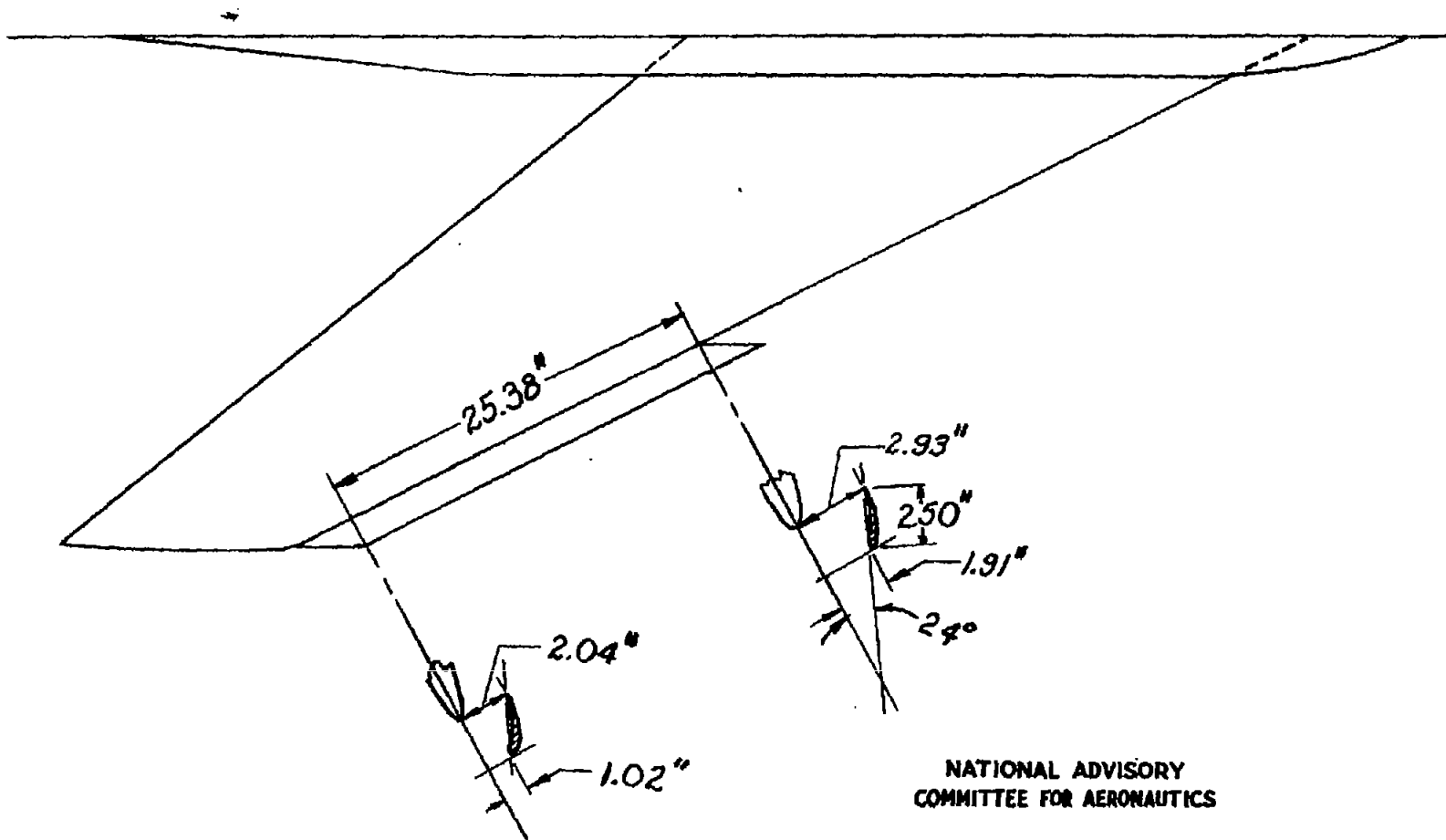
NATIONAL ADVISORY
COMMITTEE FOR AERONAUTICS

Figure 5.- Leading-edge extension 2. Area of extension,
1.70 square feet.



NATIONAL ADVISORY
COMMITTEE FOR AERONAUTICS

Figure 6.- Trailing-edge extension. Area of extension,
1.11 square feet.



NATIONAL ADVISORY
COMMITTEE FOR AERONAUTICS

Figure 7.- Partial-span slat 1.

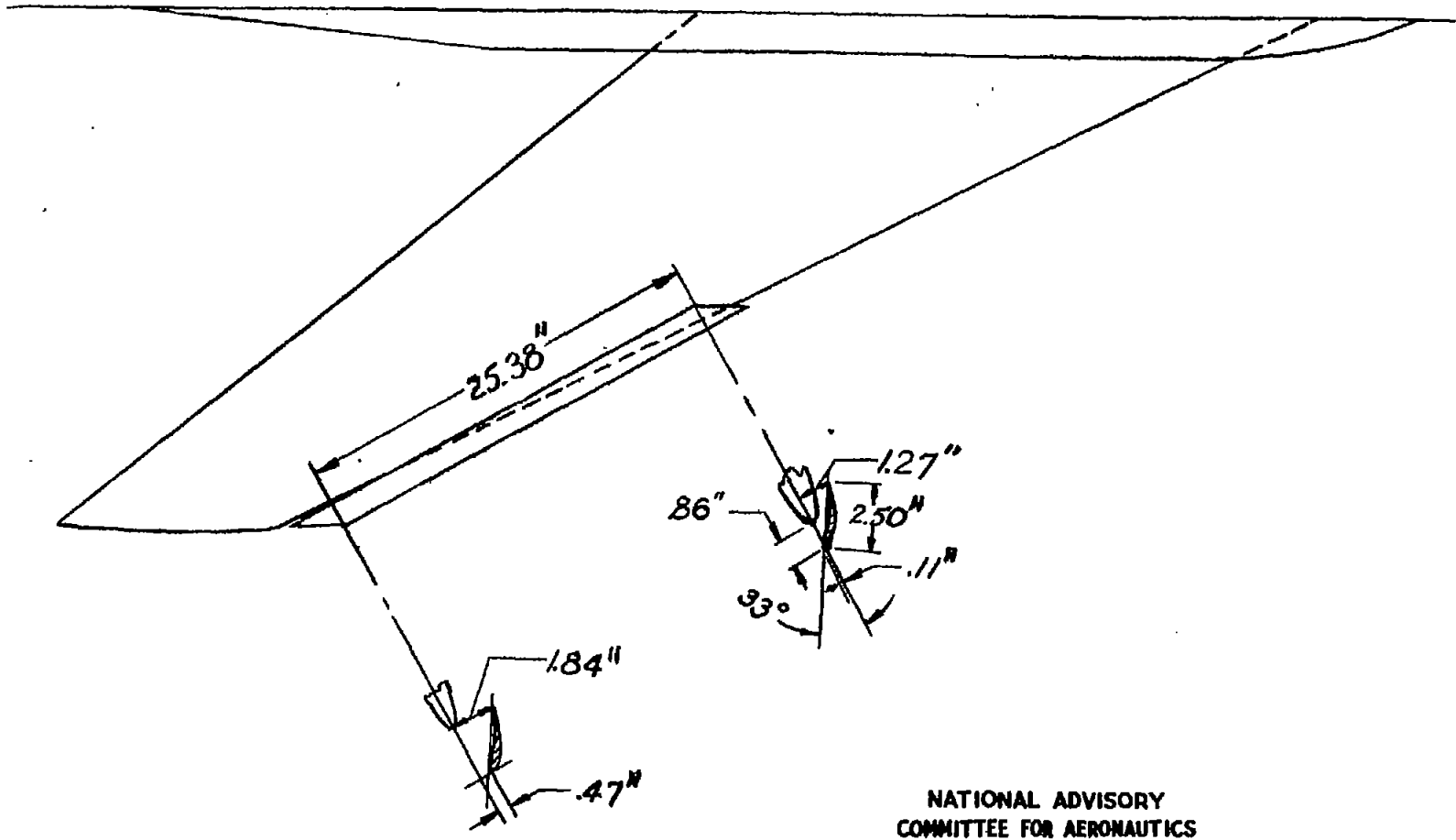
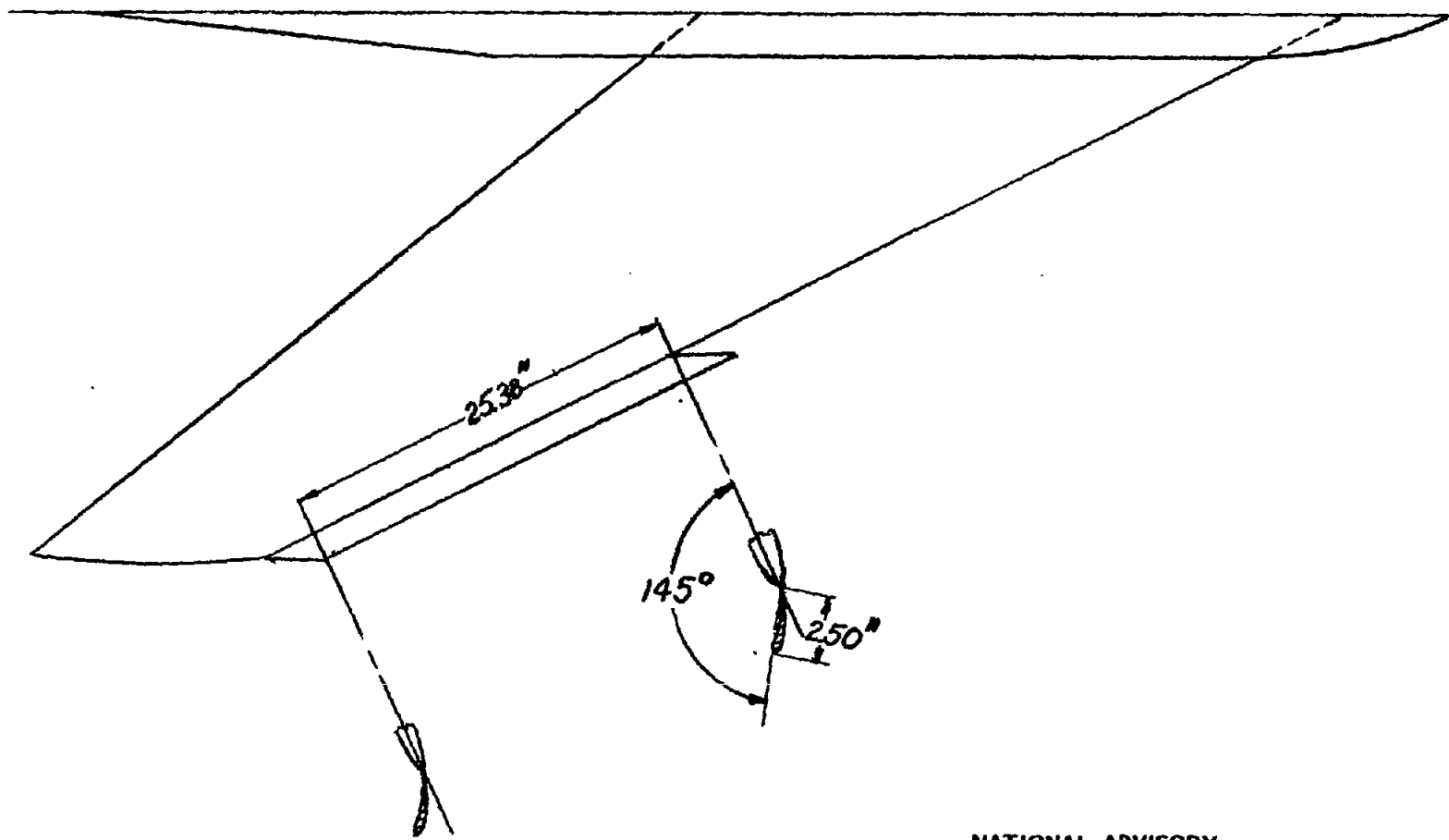


Figure 8.- Partial-span slat 2.

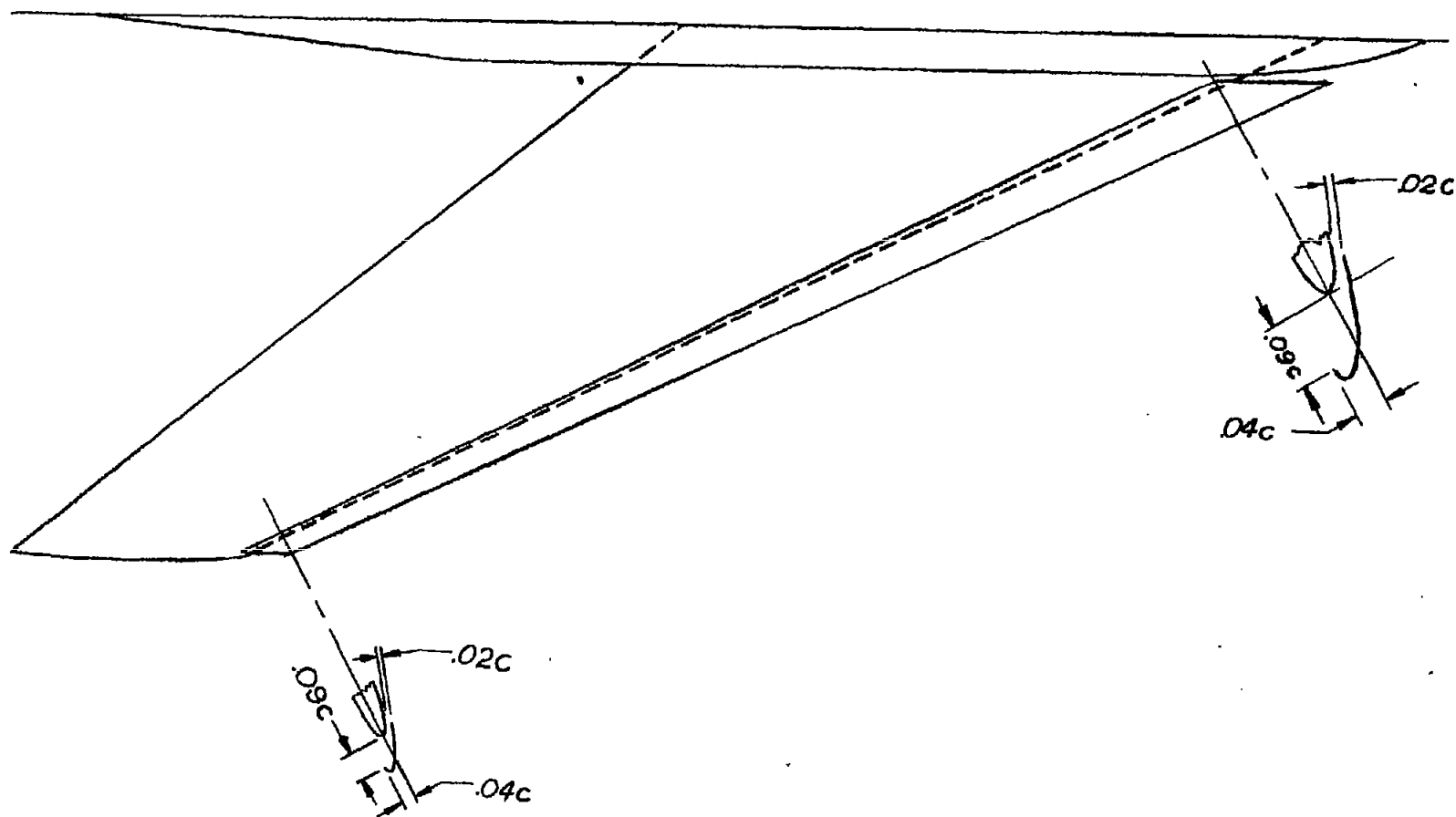
Fig. 9



NATIONAL ADVISORY
COMMITTEE FOR AERONAUTICS

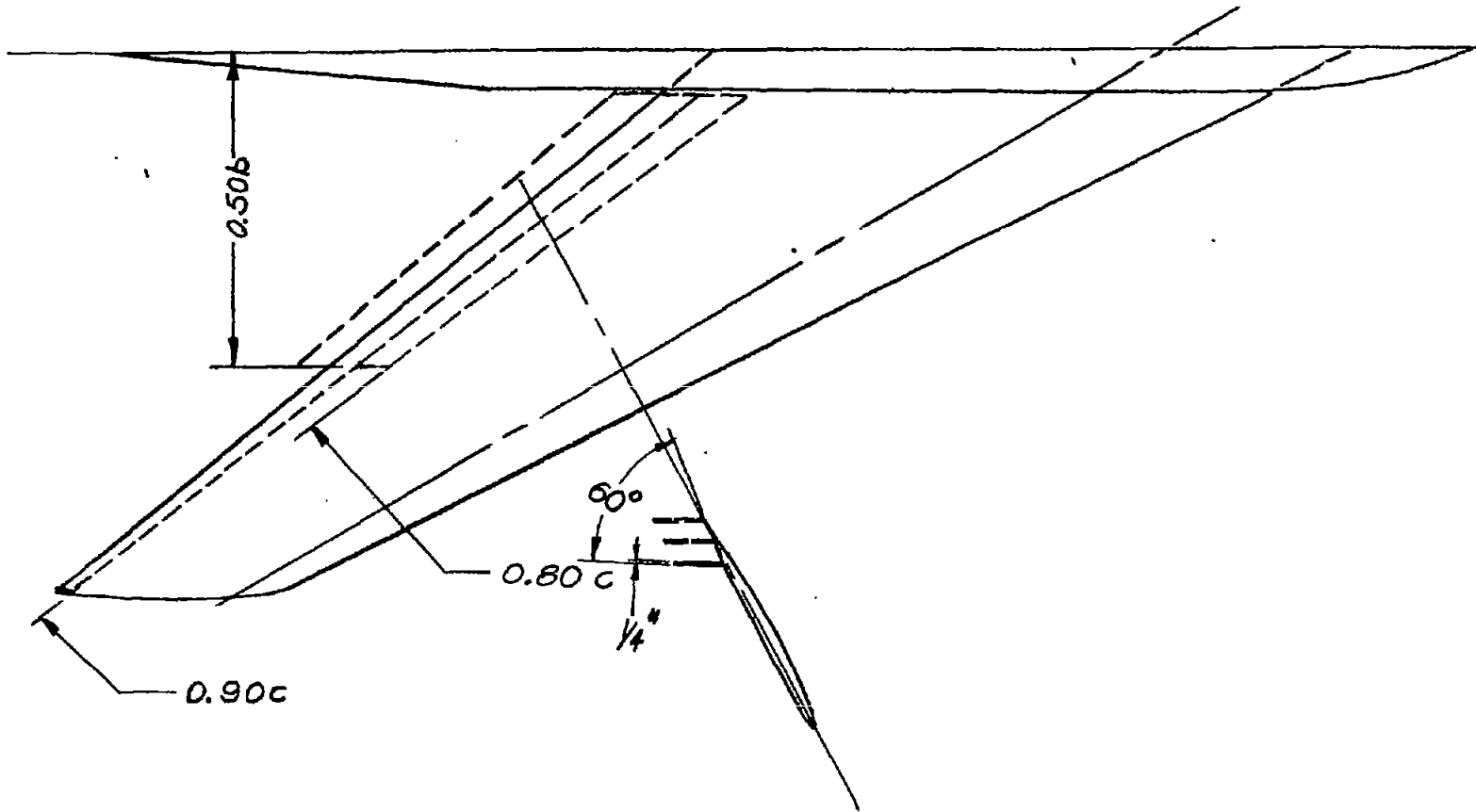
Figure 9.- Leading-edge flap.

NACA TN No. 1284



NATIONAL ADVISORY
COMMITTEE FOR AERONAUTICS

Figure 10.- Full-span slat.



NATIONAL ADVISORY
COMMITTEE FOR AERONAUTICS

Figure 11.- The 0.20-chord split-type flap deflected 60° about the 0.80, 0.90, and 1.00 chord line.

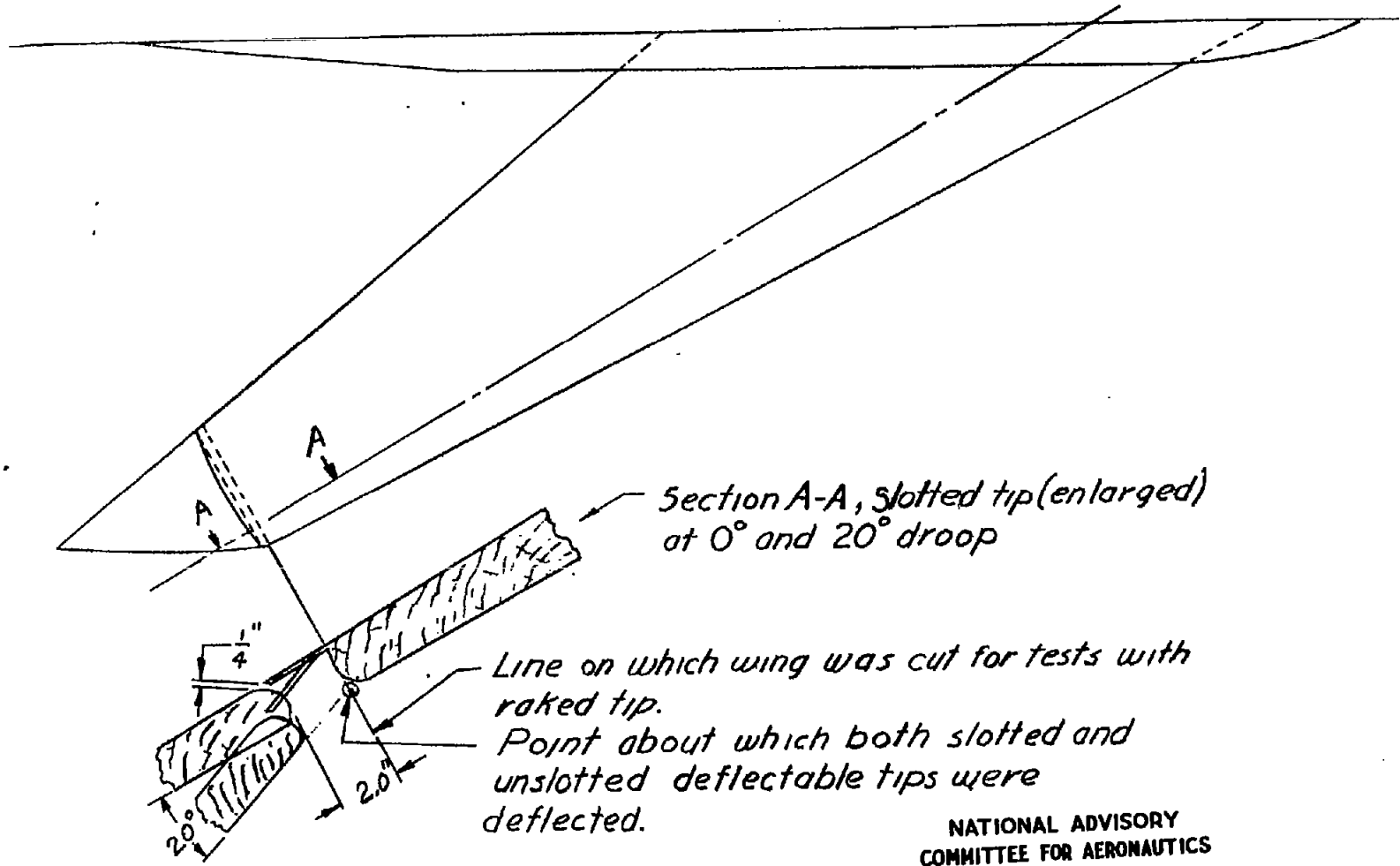
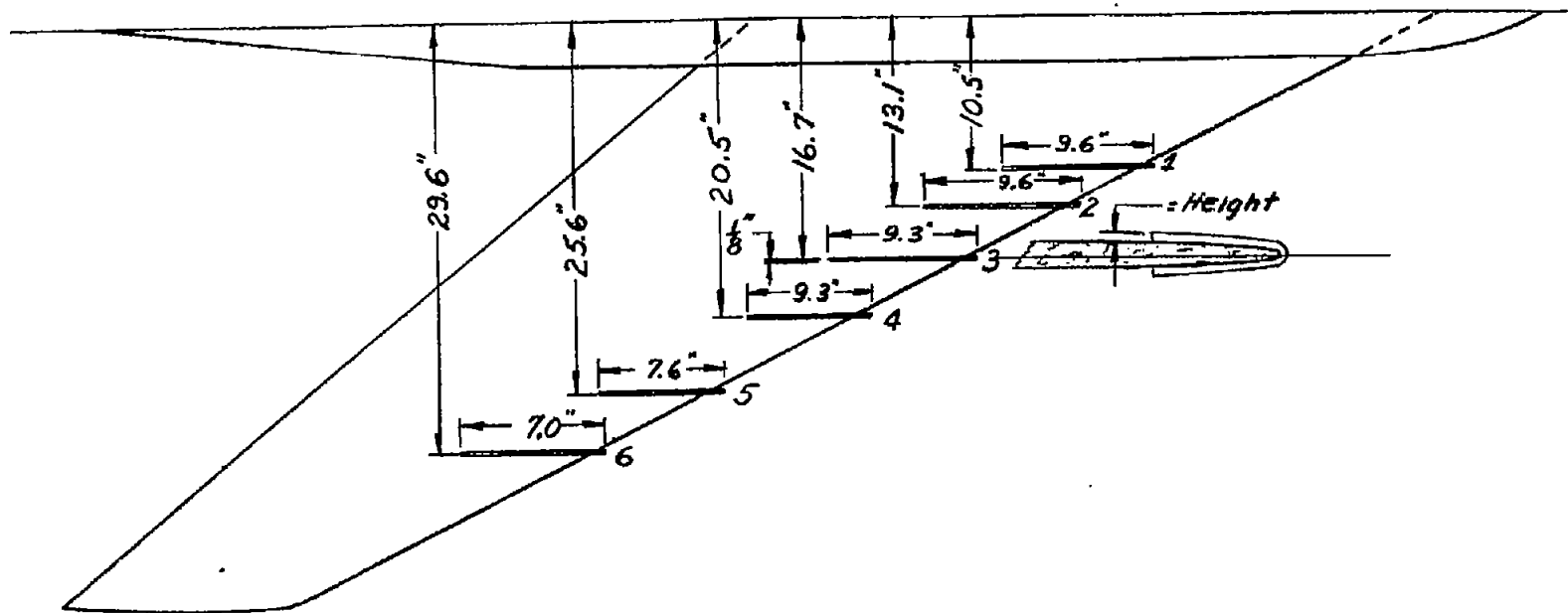


Figure 12.- Raked and deflectable tip.



NATIONAL ADVISORY
COMMITTEE FOR AERONAUTICS

Figure 13.- Six leading-edge deflector plates. Height of plates 1, 2, 5, and 6, 1/2 inch; height of plates 3 and 4, 1 inch.

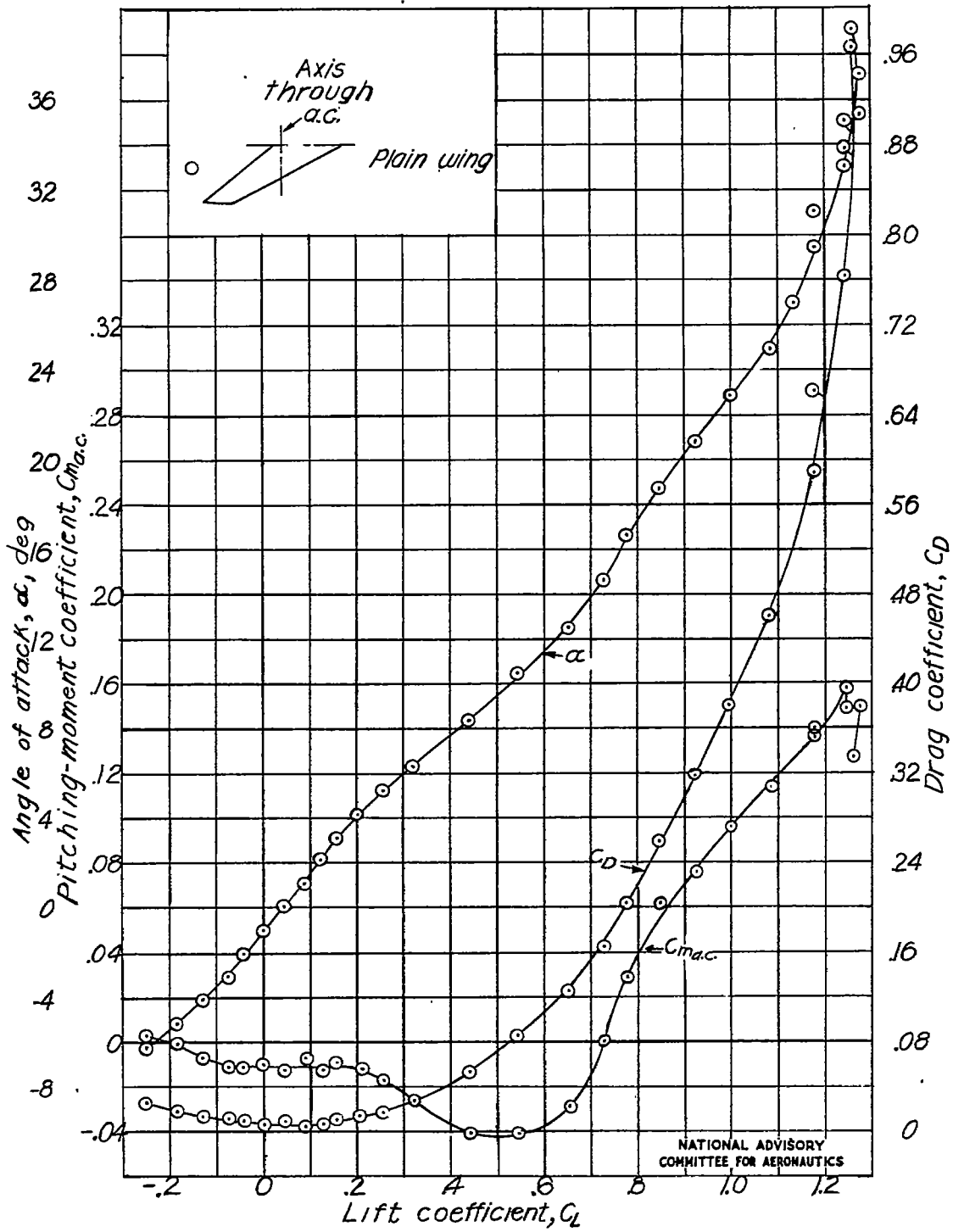


Figure 14.- Aerodynamic characteristics of 60° swept-back wing. $q = 20.1$ pounds per square foot.

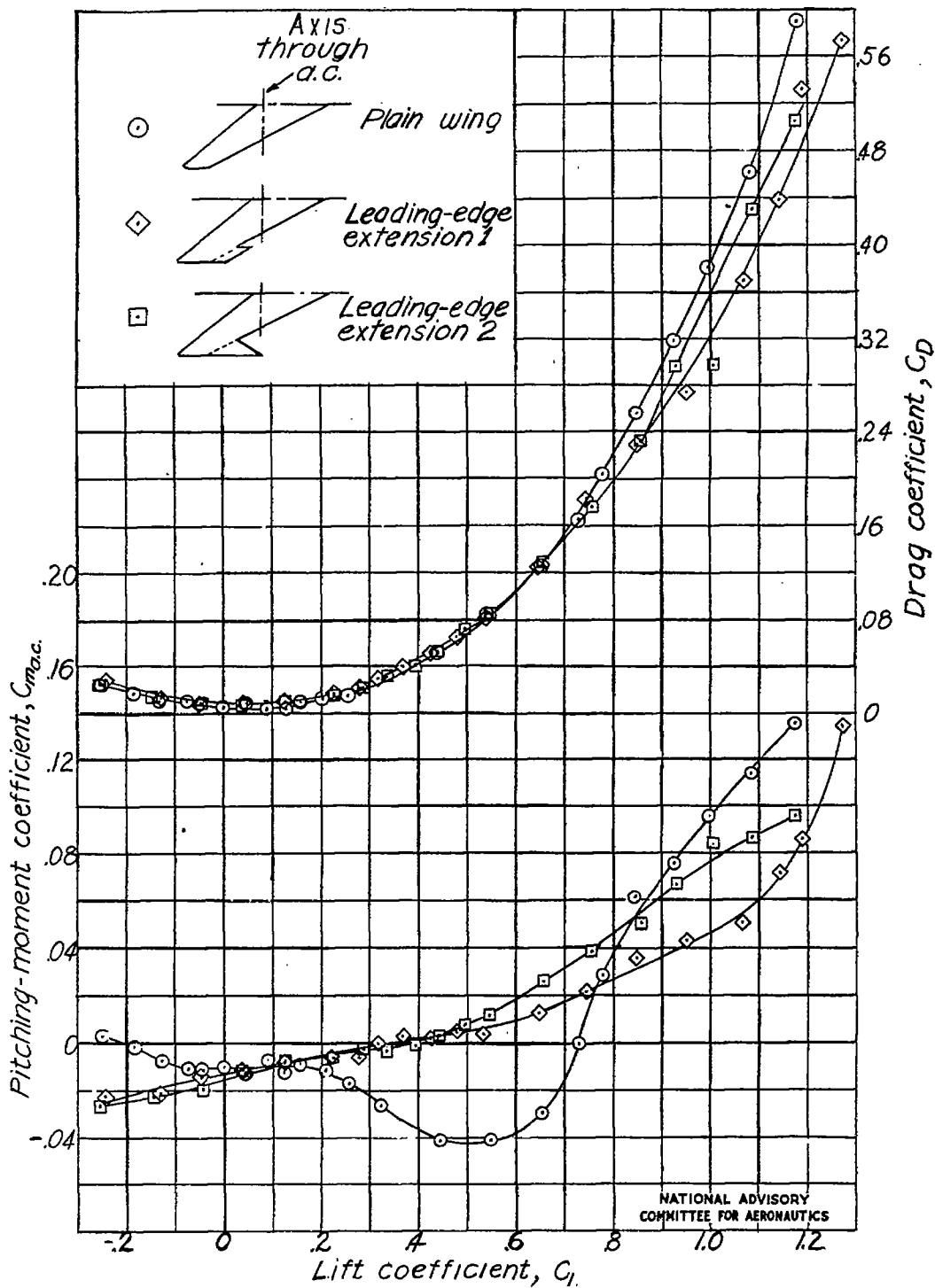


Figure 15.- Aerodynamic characteristics of 60° swept-back wing with and without leading-edge extensions. $q = 20.1$ pounds per square foot.

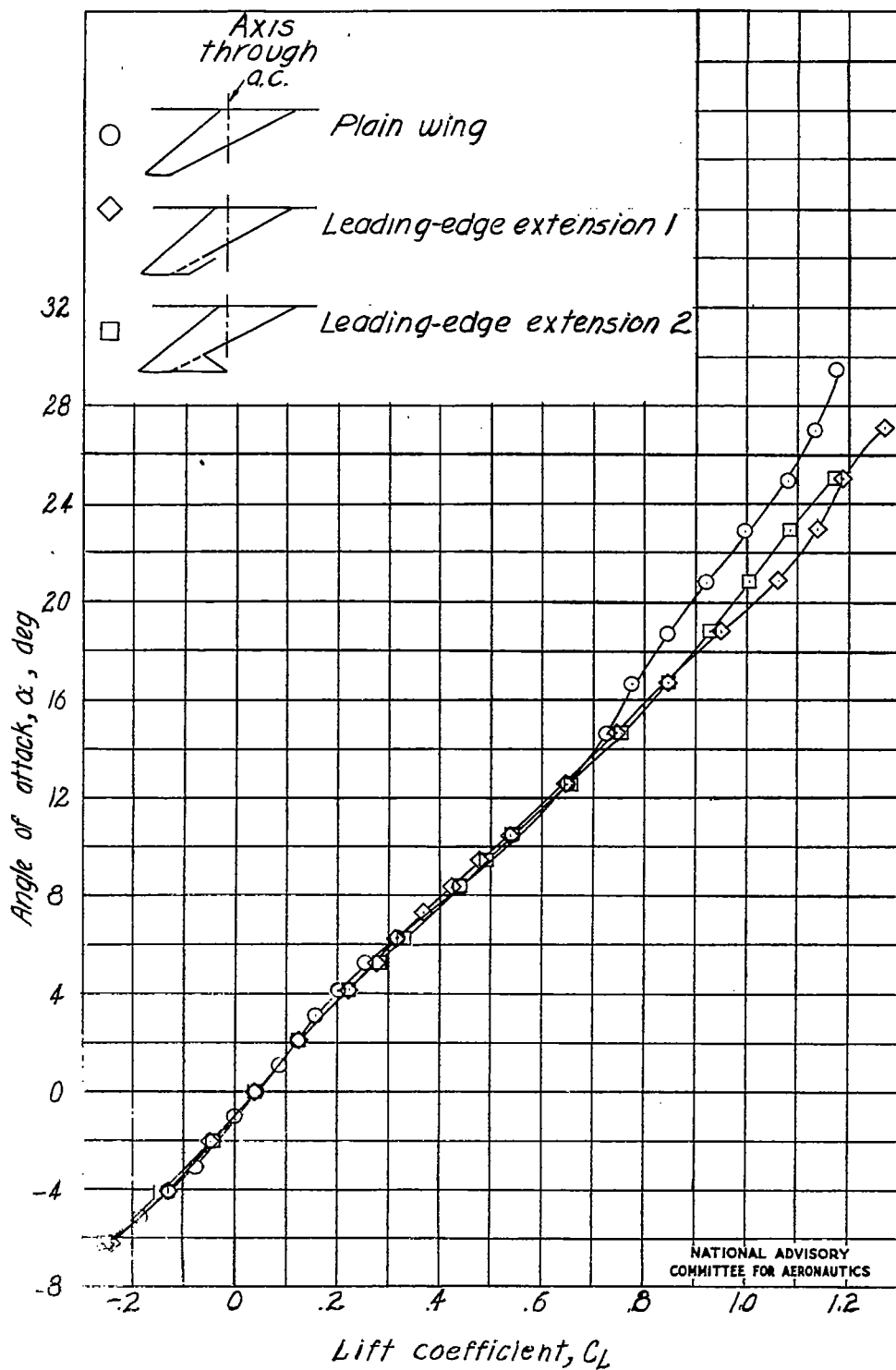


Figure 15.- Concluded.

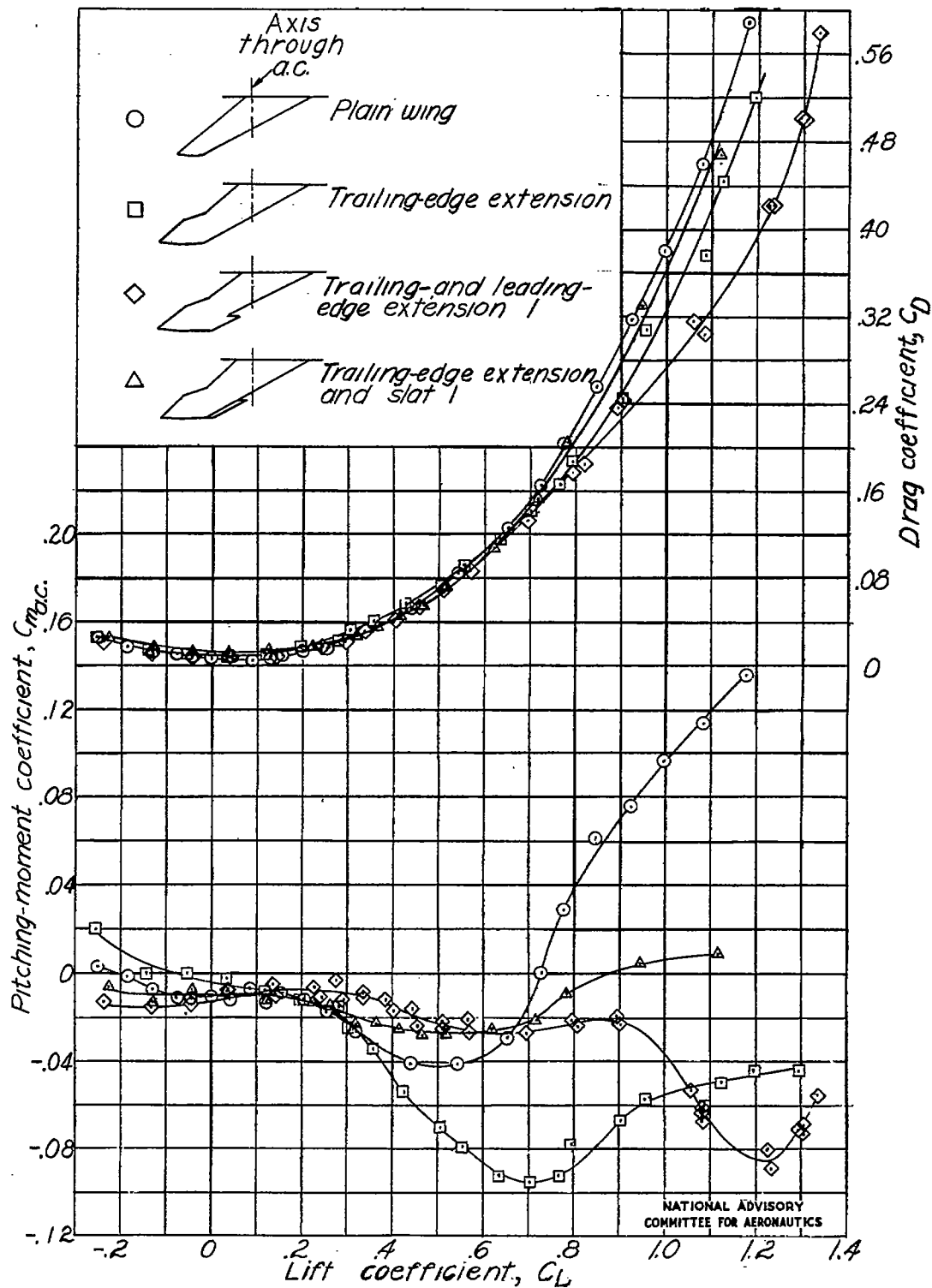


Figure 16.- Aerodynamic characteristics of 60° swept-back wing with several combinations of a leading- and a trailing-edge extension and slot 1. $q = 20.1$ pounds per square foot.

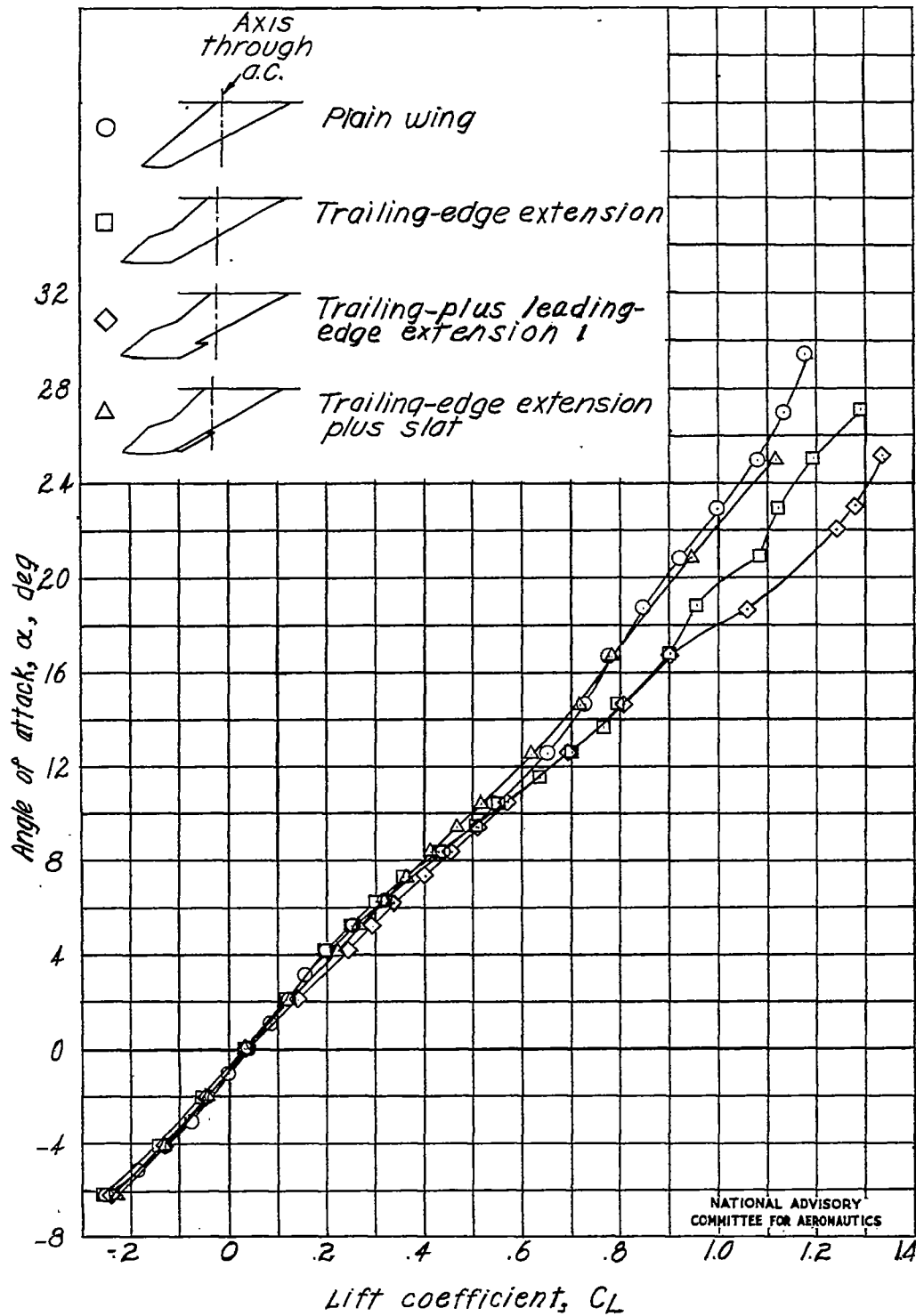


Figure 16.- Concluded.

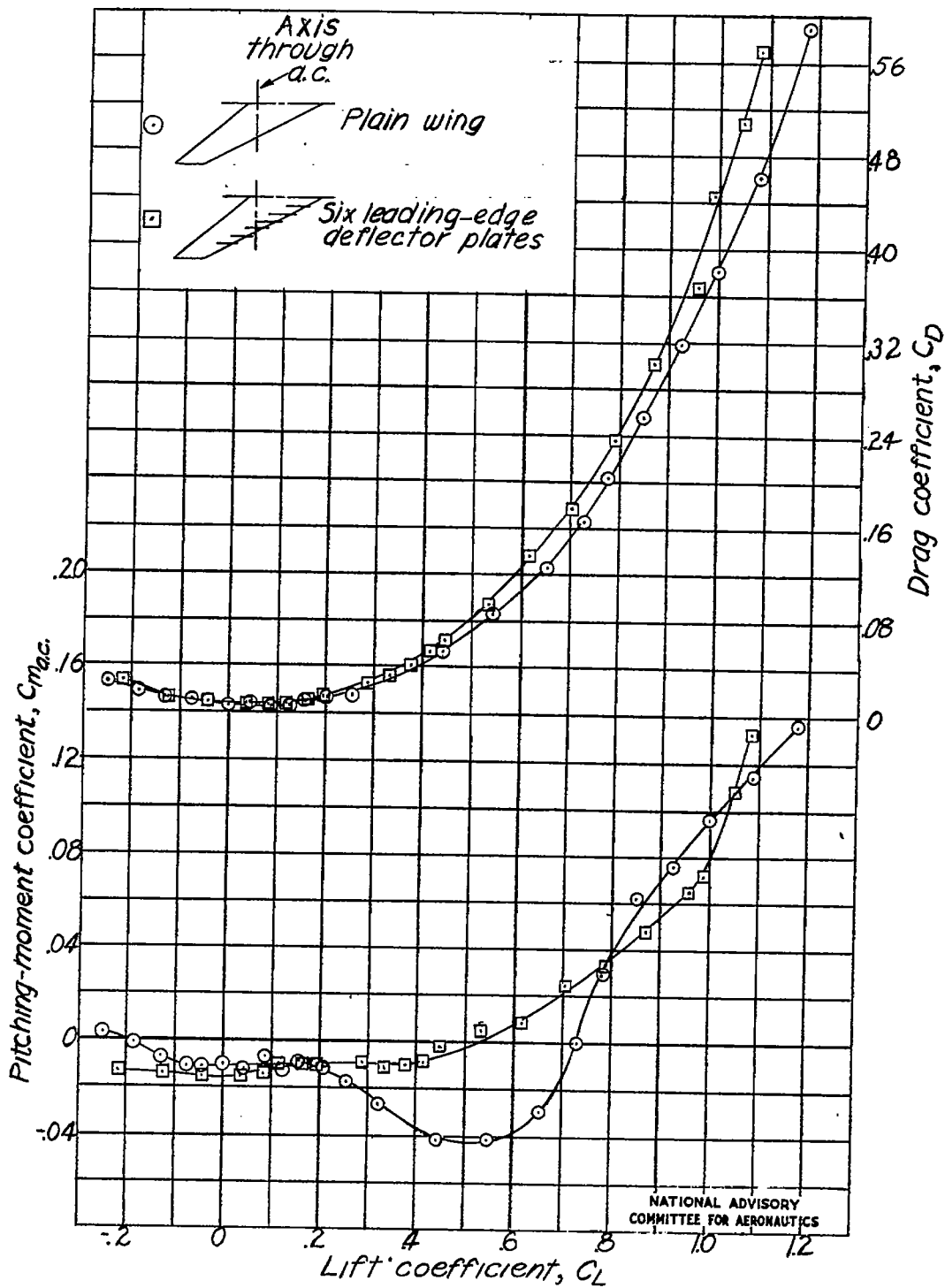


Figure 17.- Aerodynamic characteristics of 60° swept-back wing with and without 6 leading-edge deflector plates. $q = 20.1$ pounds per square foot.

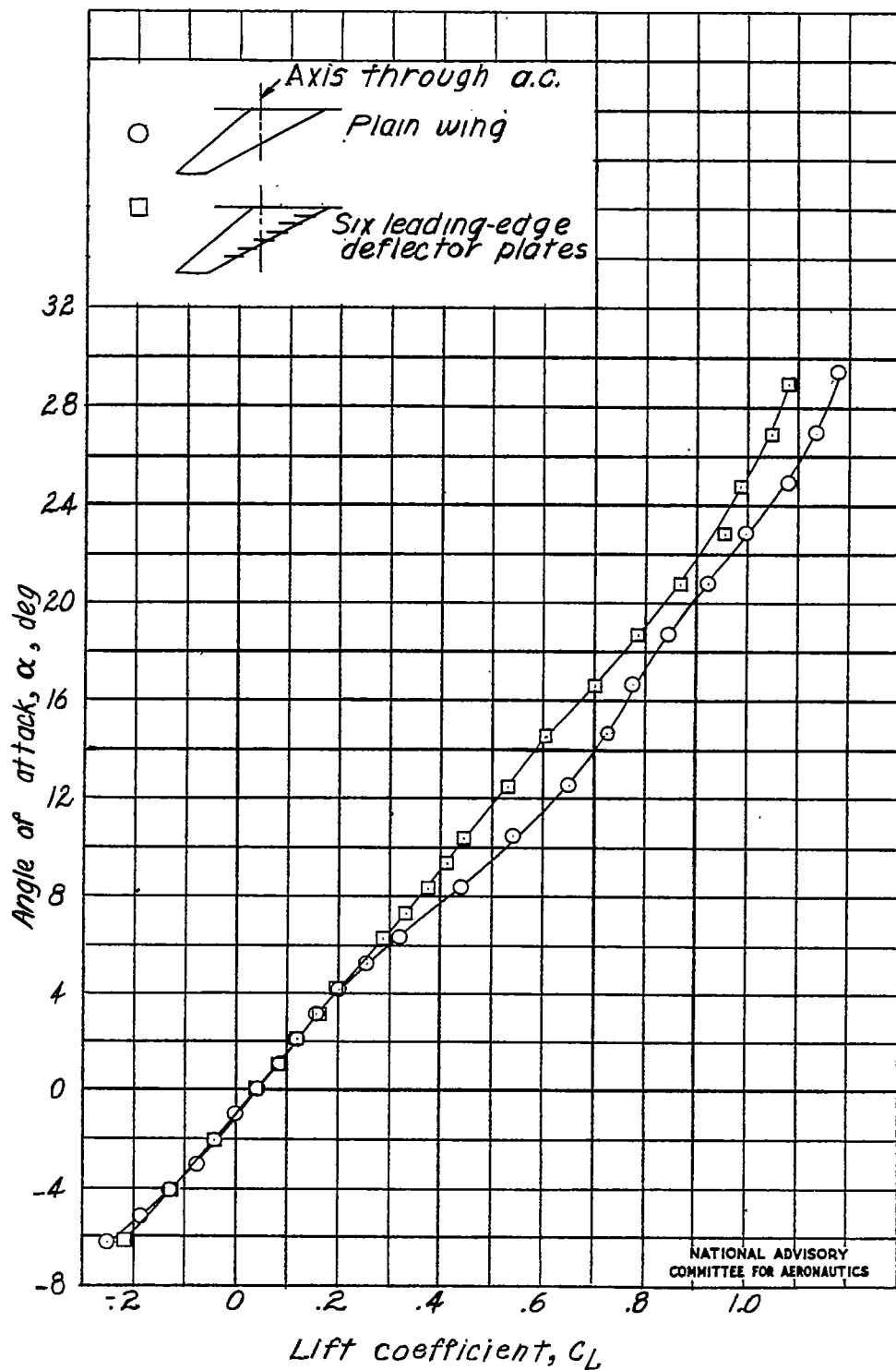


Figure 17.- Concluded.

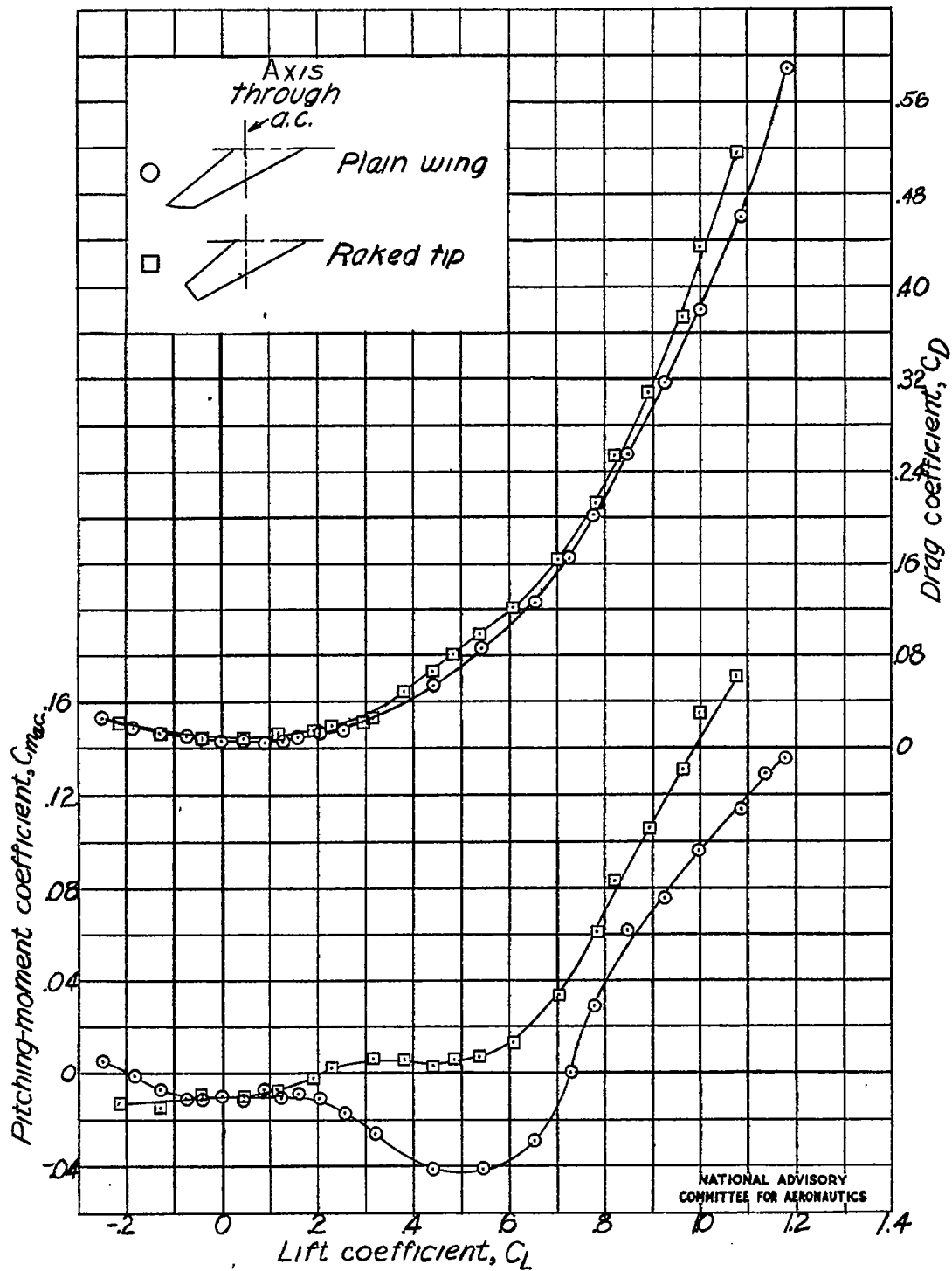


Figure 18.- Aerodynamic characteristics of 60° swept-back wing with original and raked tip. $q = 20.1$ pounds per square foot.

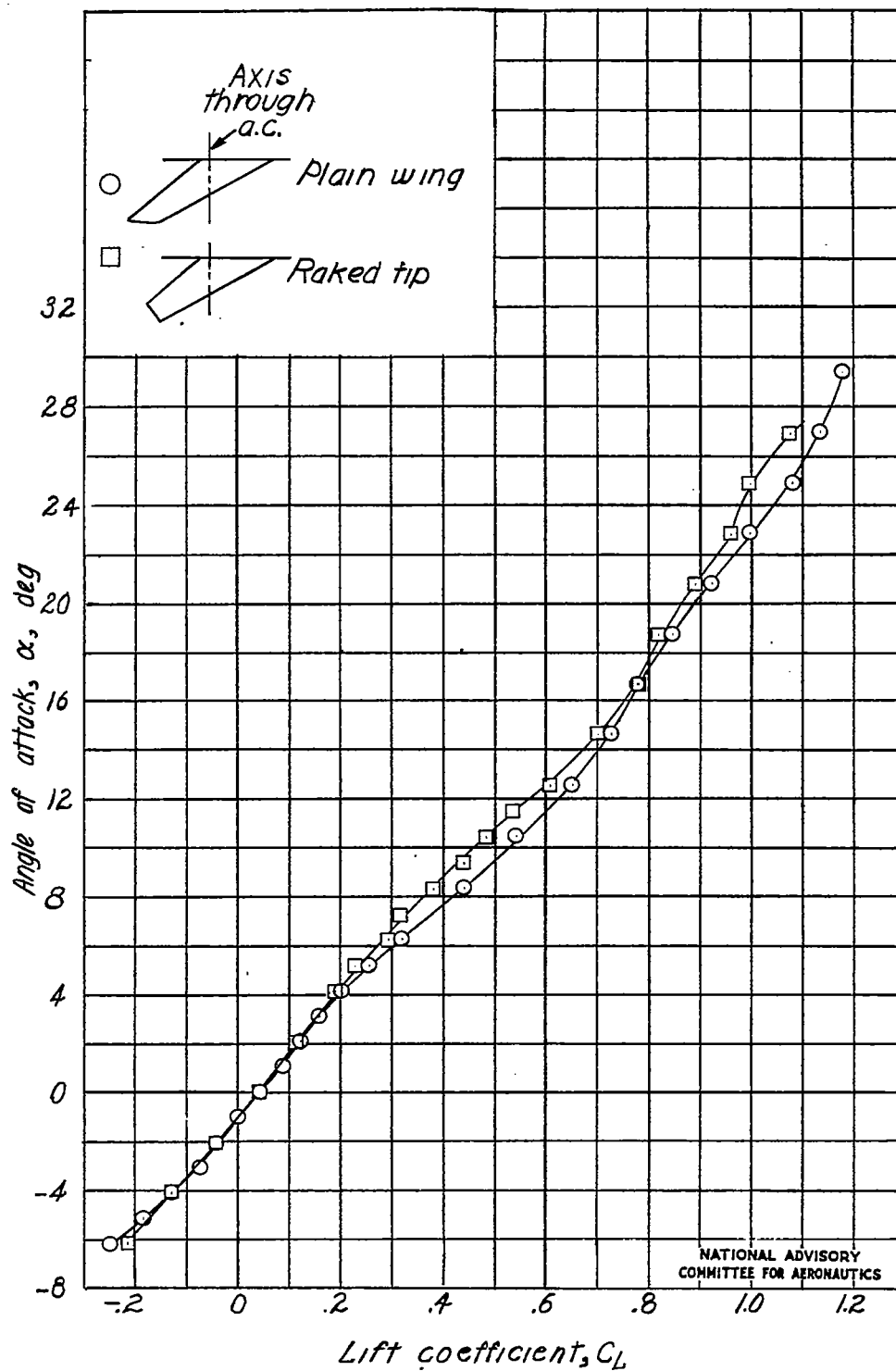


Figure 18.- Concluded.

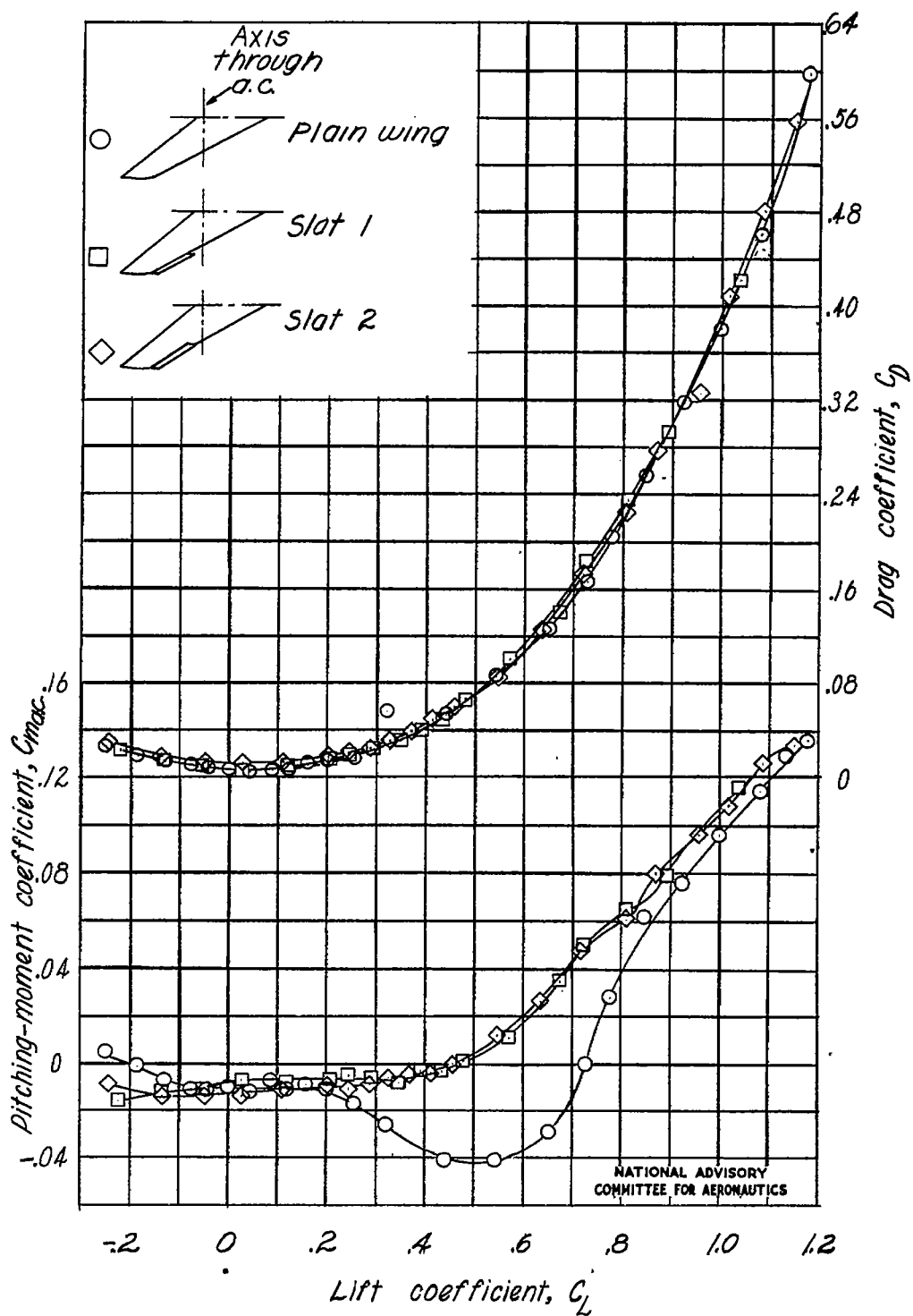


Figure 19.- Aerodynamic characteristics of 60° swept-back wing with and without partial-span slat. $q = 20.1$ pounds per square foot.

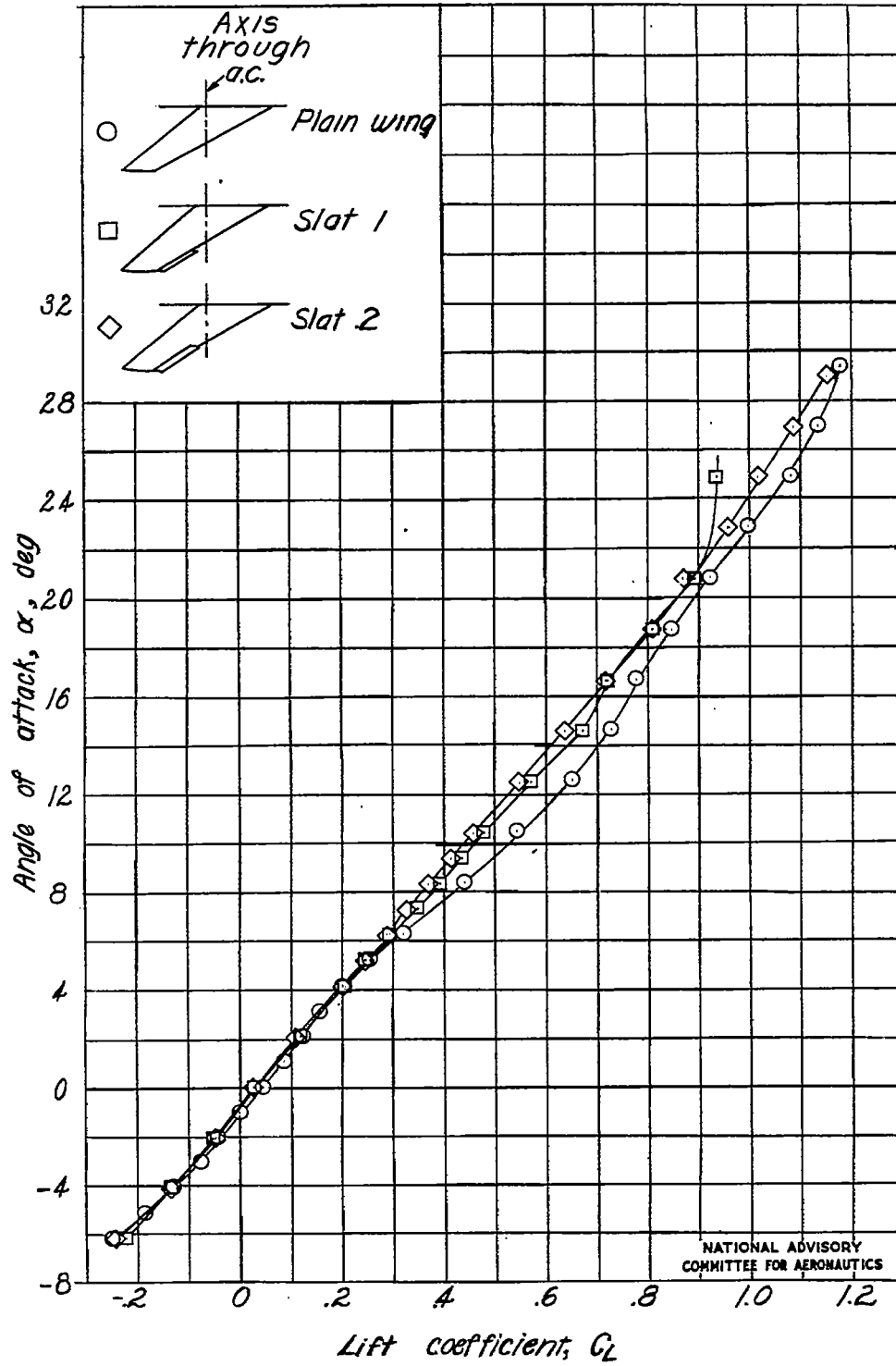


Figure 19.- Concluded.

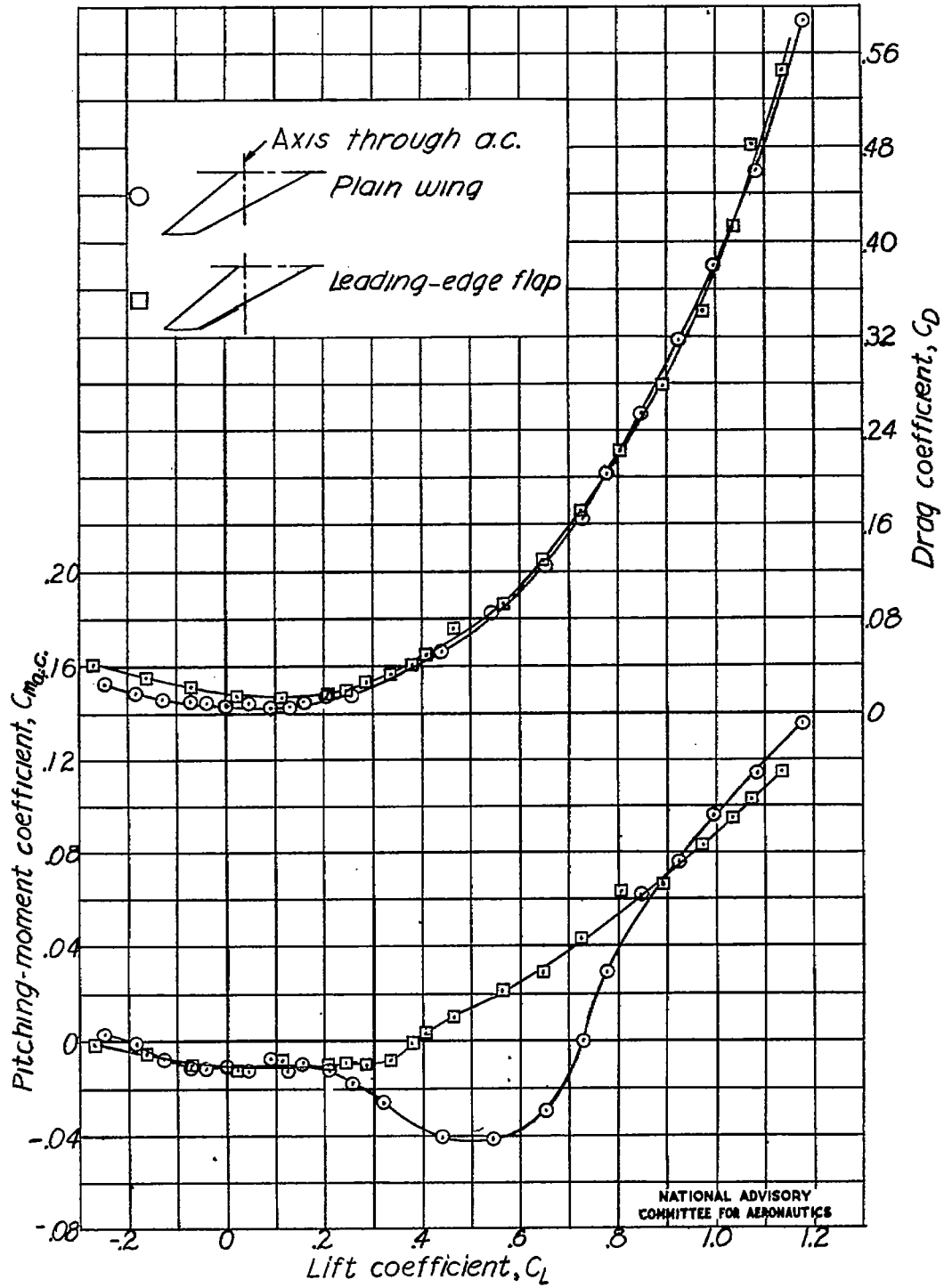


Figure 20.- Aerodynamic characteristics of 60° swept-back wing with and without leading-edge flap. $q = 20.1$ pounds per square foot.

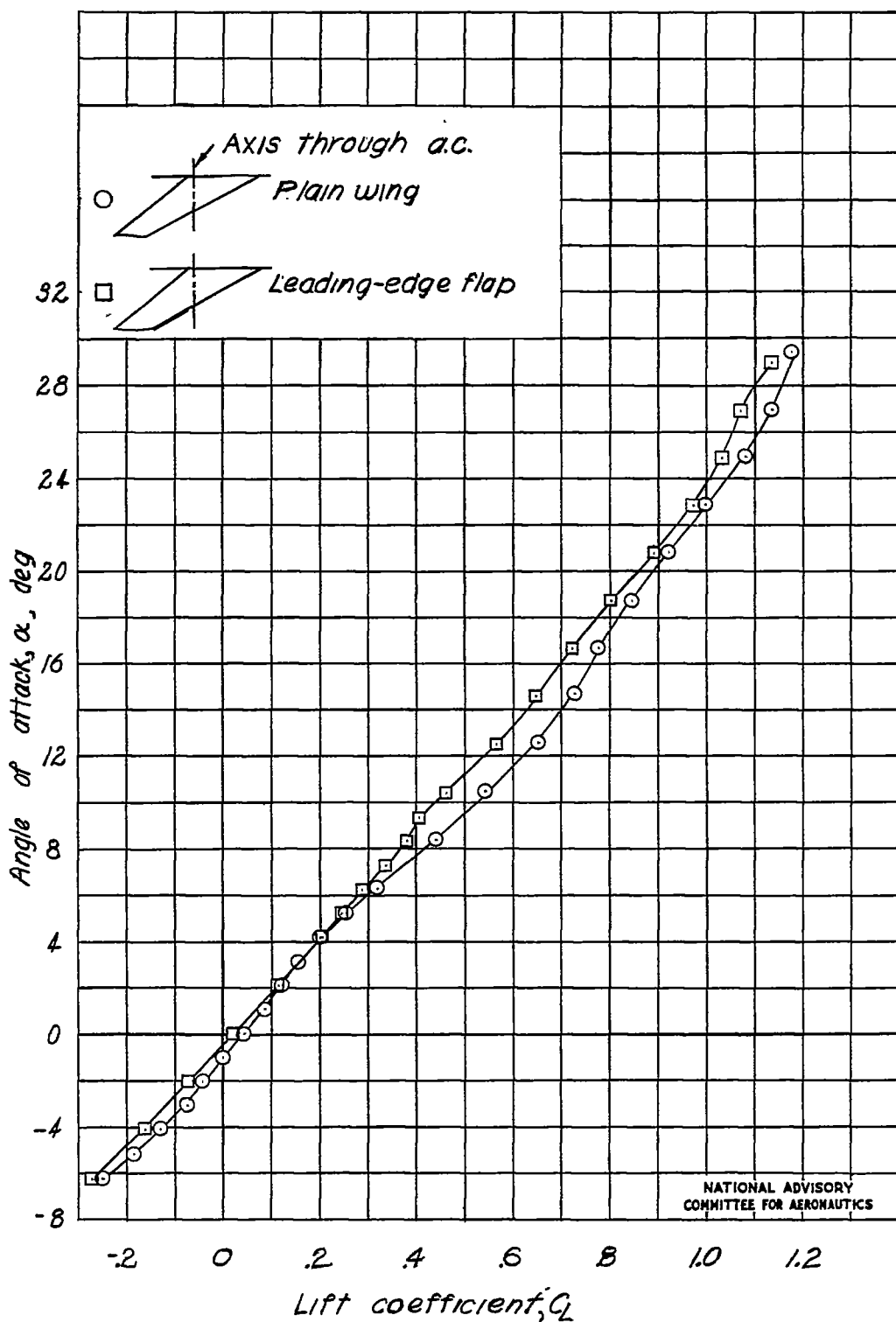


Figure 20.- Concluded.

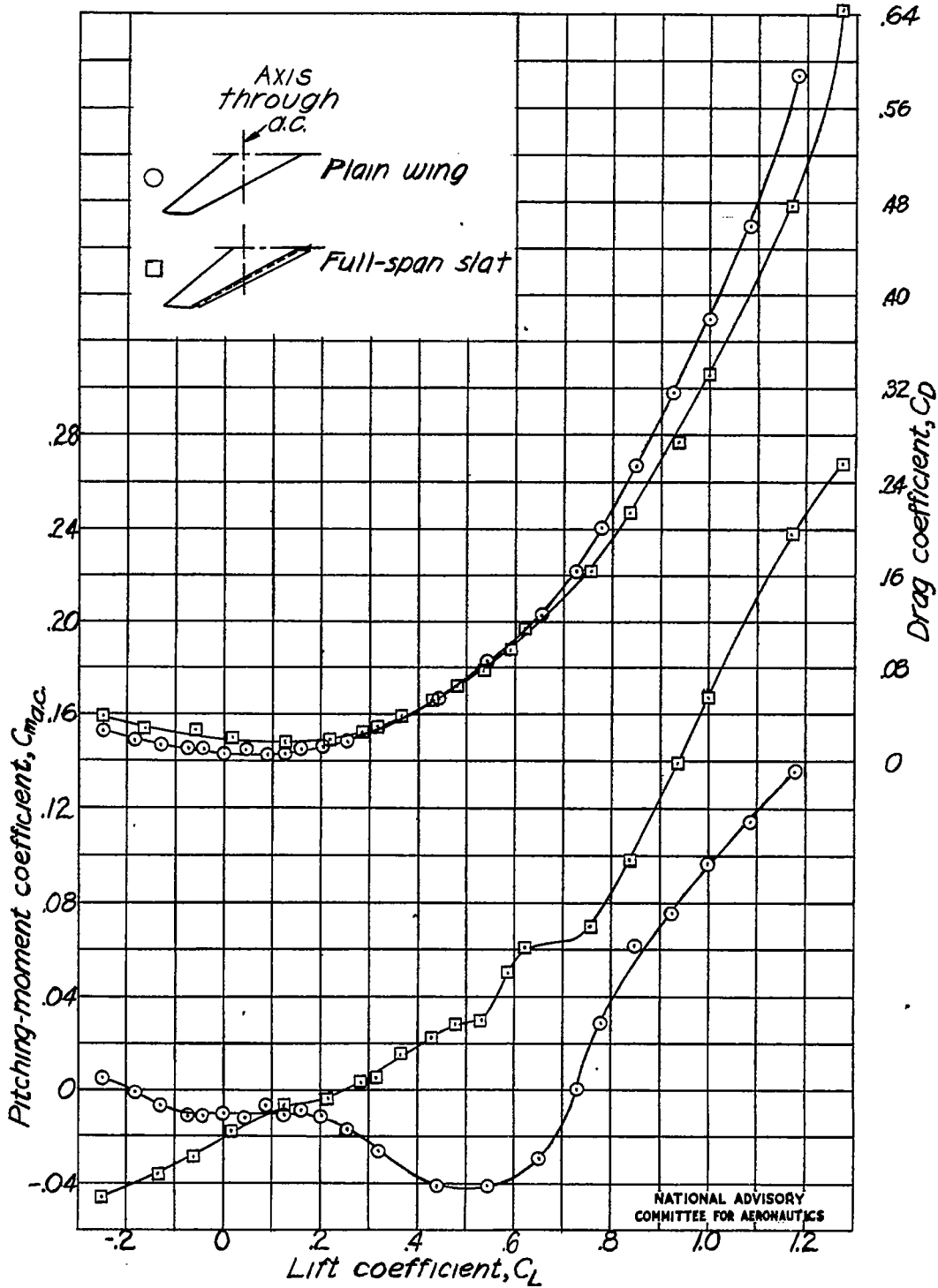


Figure 21.- Aerodynamic characteristics of 60° swept-back wing with and without full-span slat. $q = 20.1$ pounds per square foot.

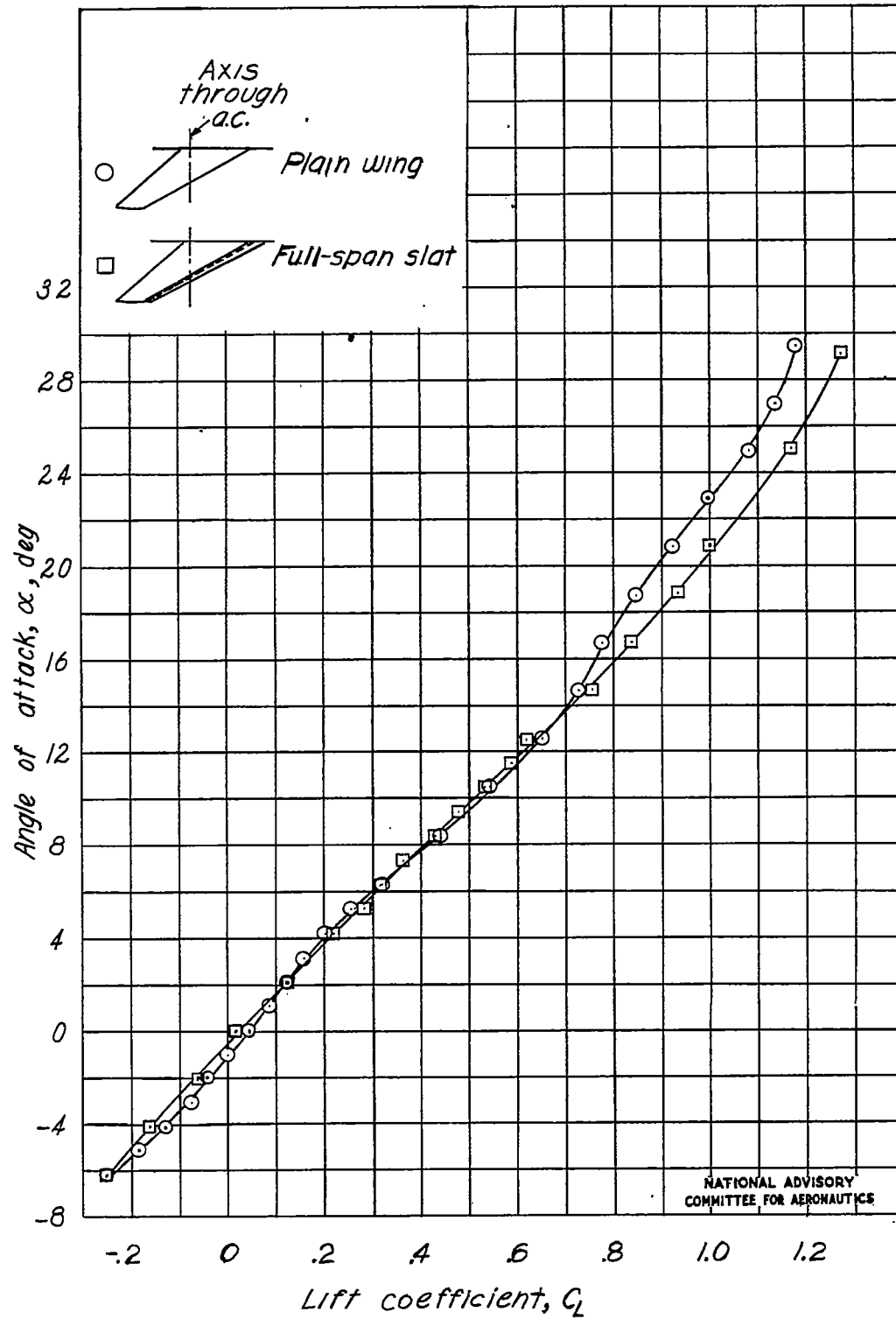


Figure 21.- Concluded.

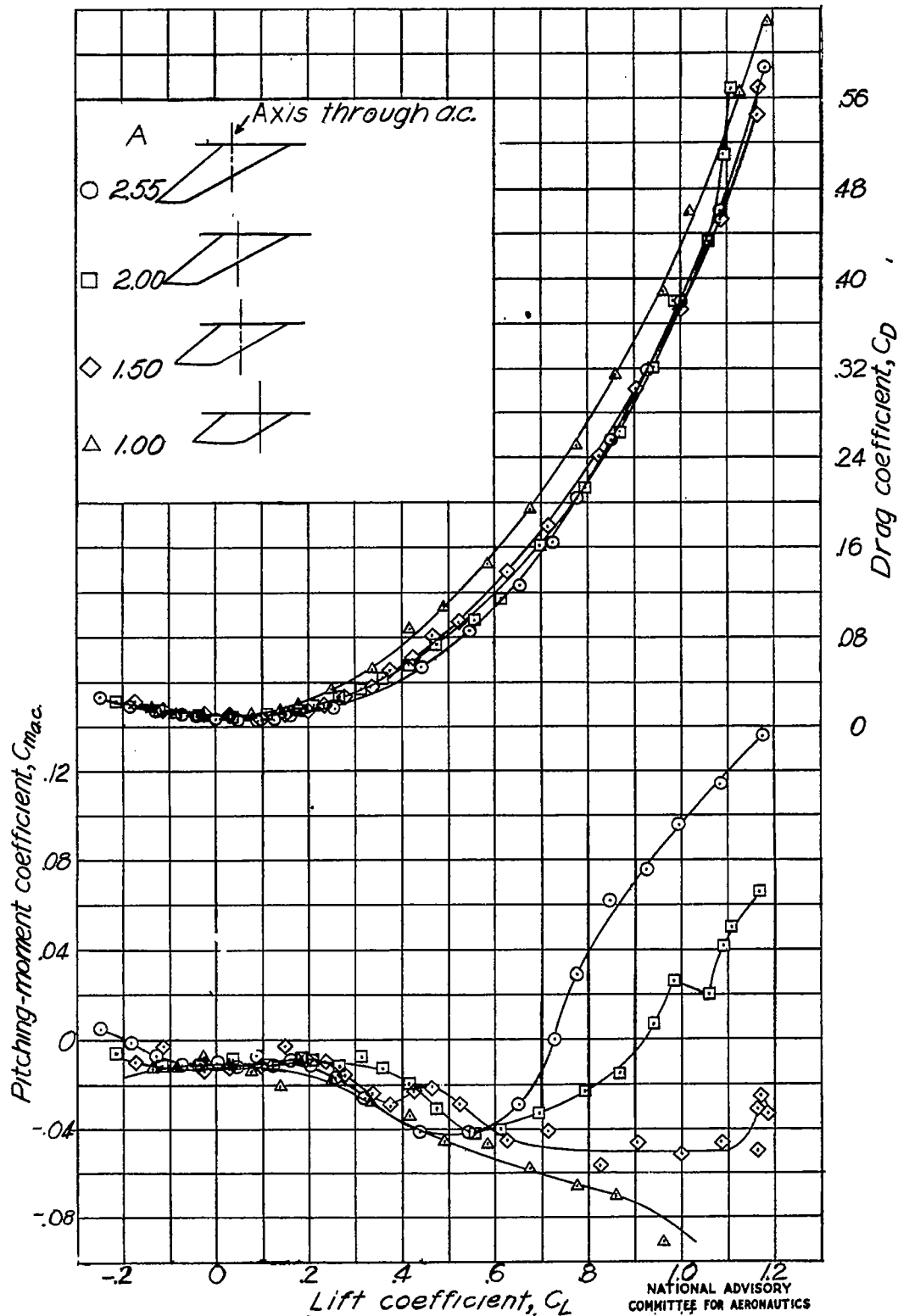


Figure 22.- Aerodynamic characteristics of 60° swept-back wings of various aspect and taper ratios. $q = 20.1$ pounds per square foot.

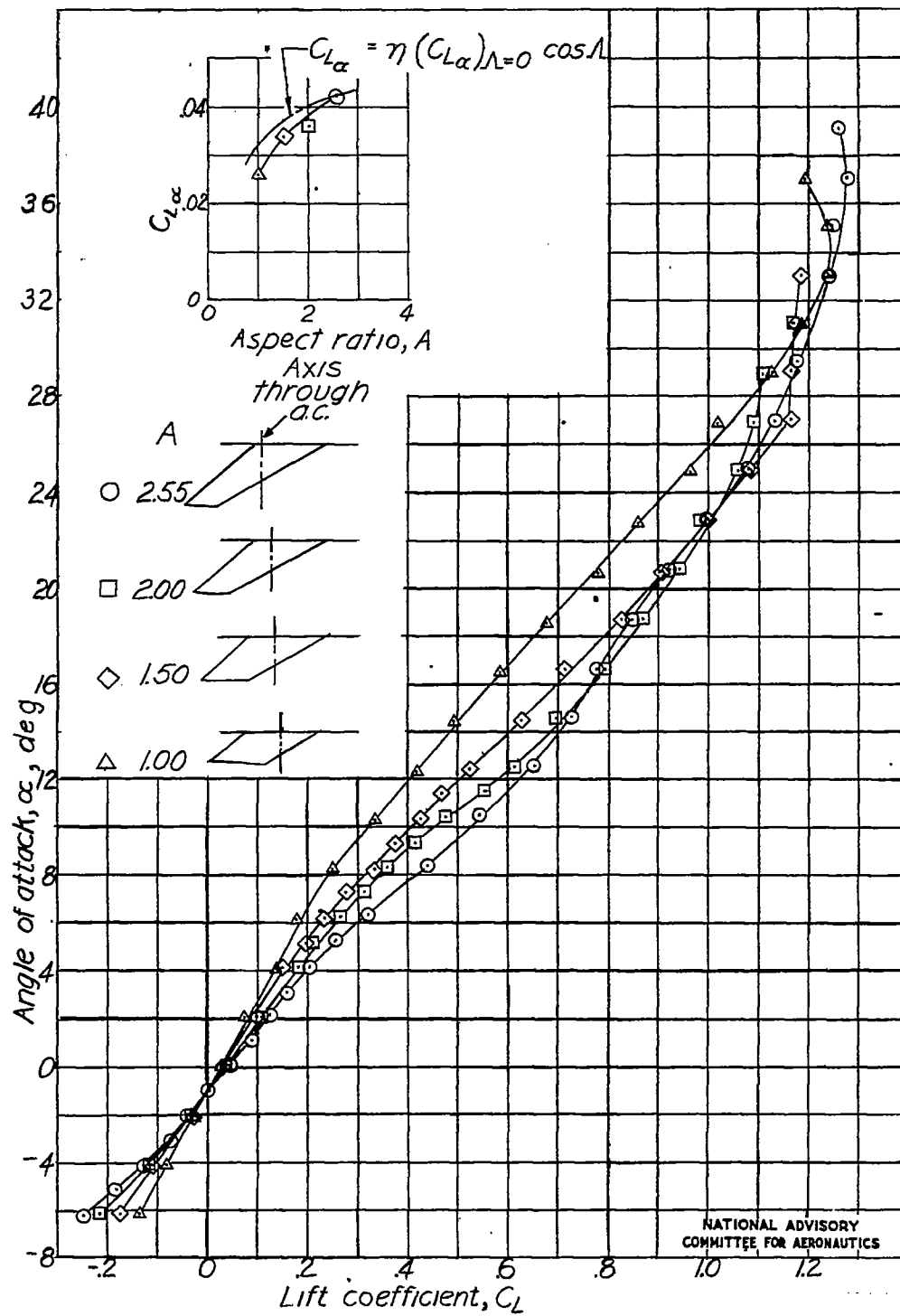


Figure 22.- Concluded.

NATIONAL ADVISORY
COMMITTEE FOR AERONAUTICS

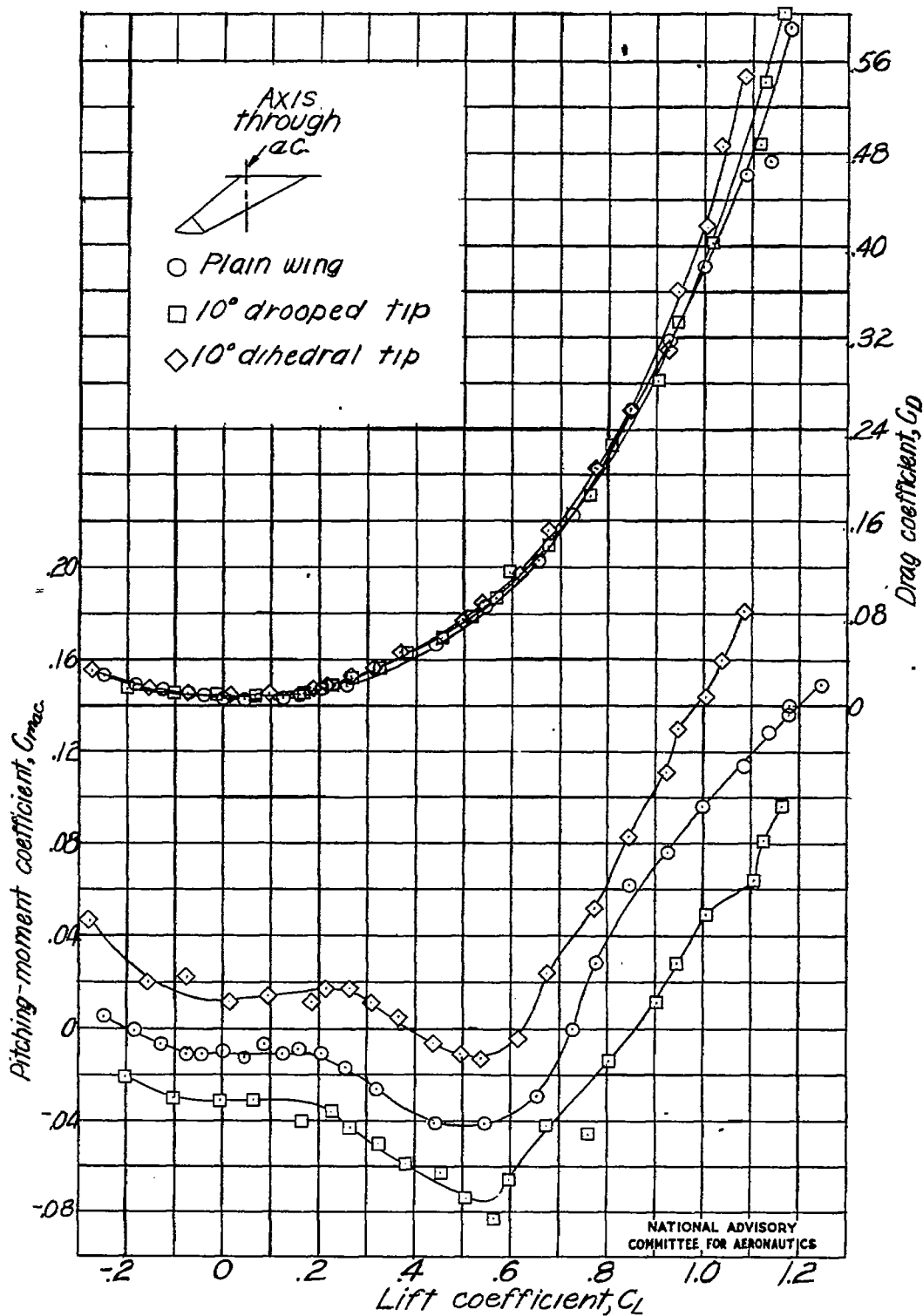


Figure 23.- Aerodynamic characteristics of 60° swept-back wing with deflectable tip, slot sealed. $q = 20.1$ pounds per square foot.

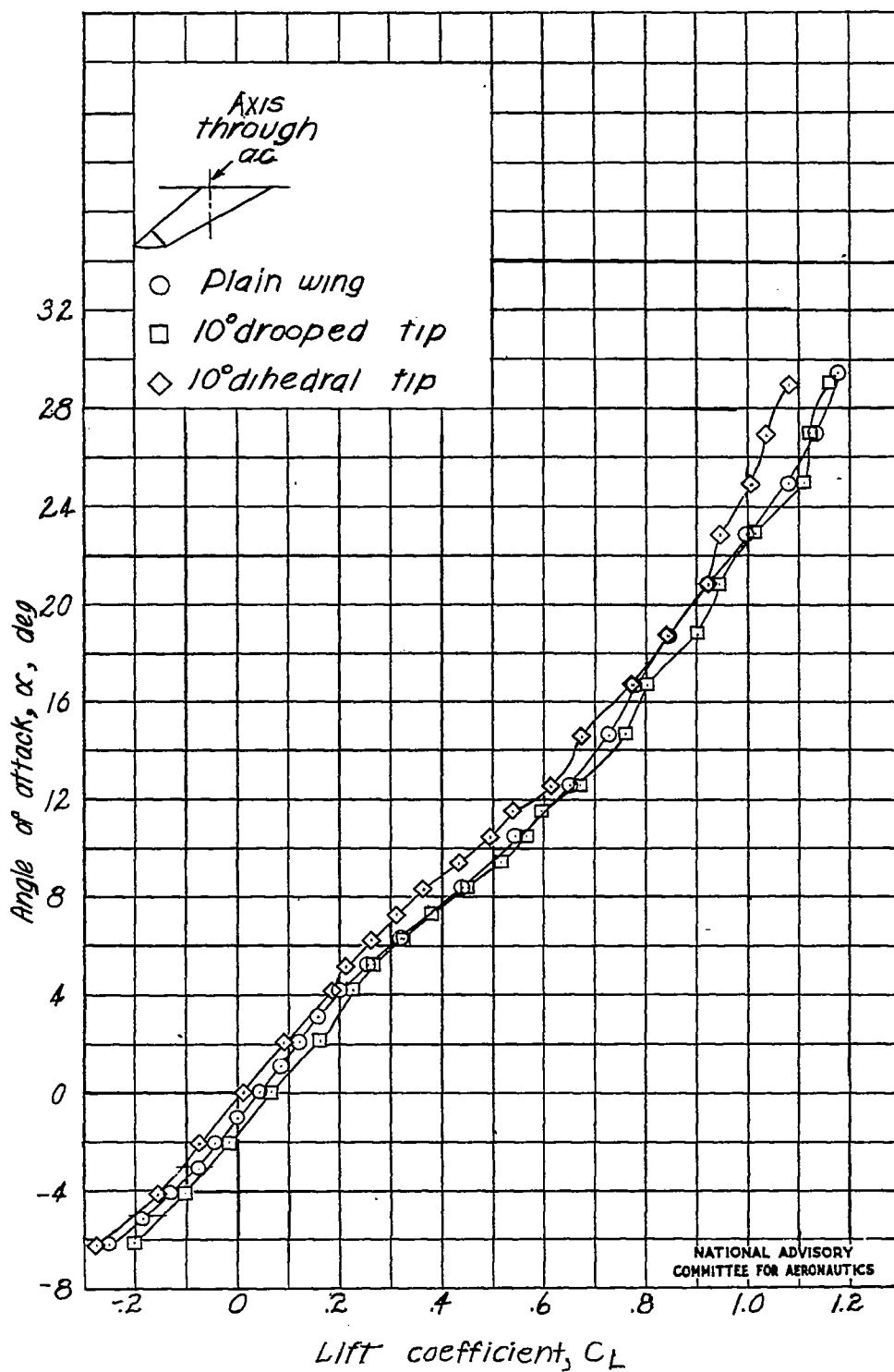


Figure 23.- Concluded.

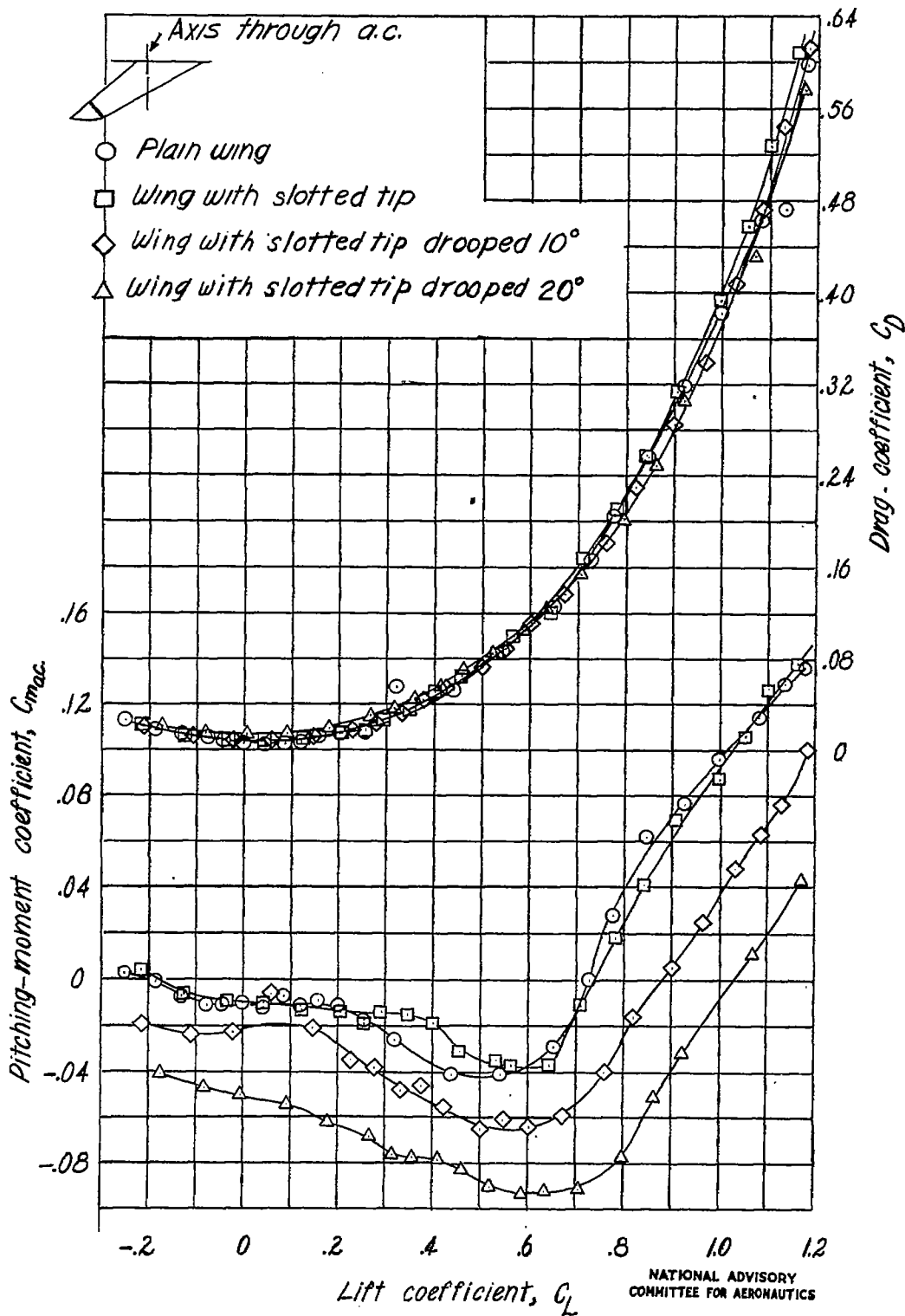


Figure 24.- Aerodynamic characteristics of 60° swept-back wing with deflectable tip, slot open. $q = 20.1$ pounds per square foot.

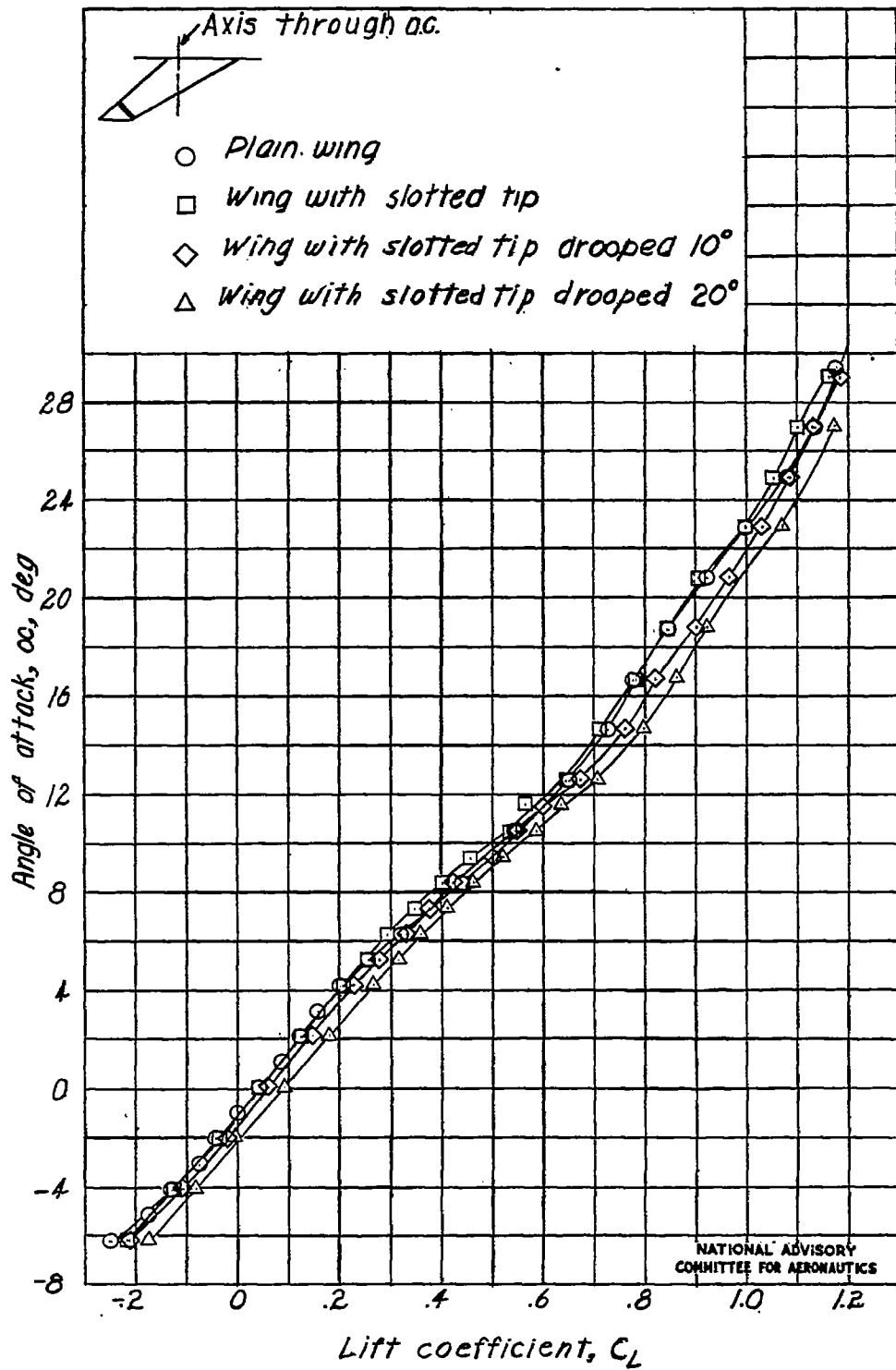


Figure 24.- Concluded.

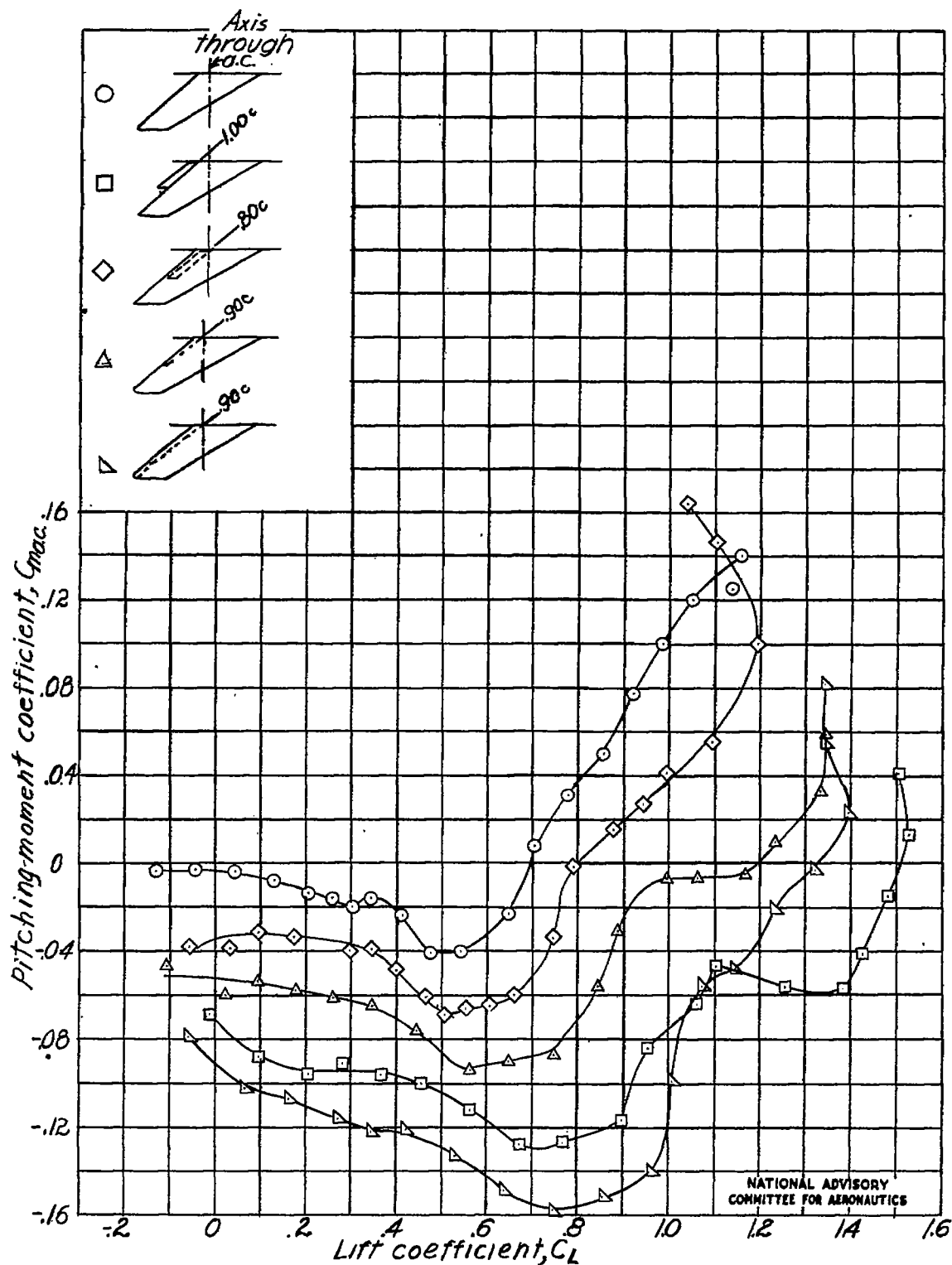


Figure 25.- Aerodynamic characteristics of 60° swept-back wing with various 0.20-chord split-type flap configurations. $q = 10.1$ pounds per square foot.

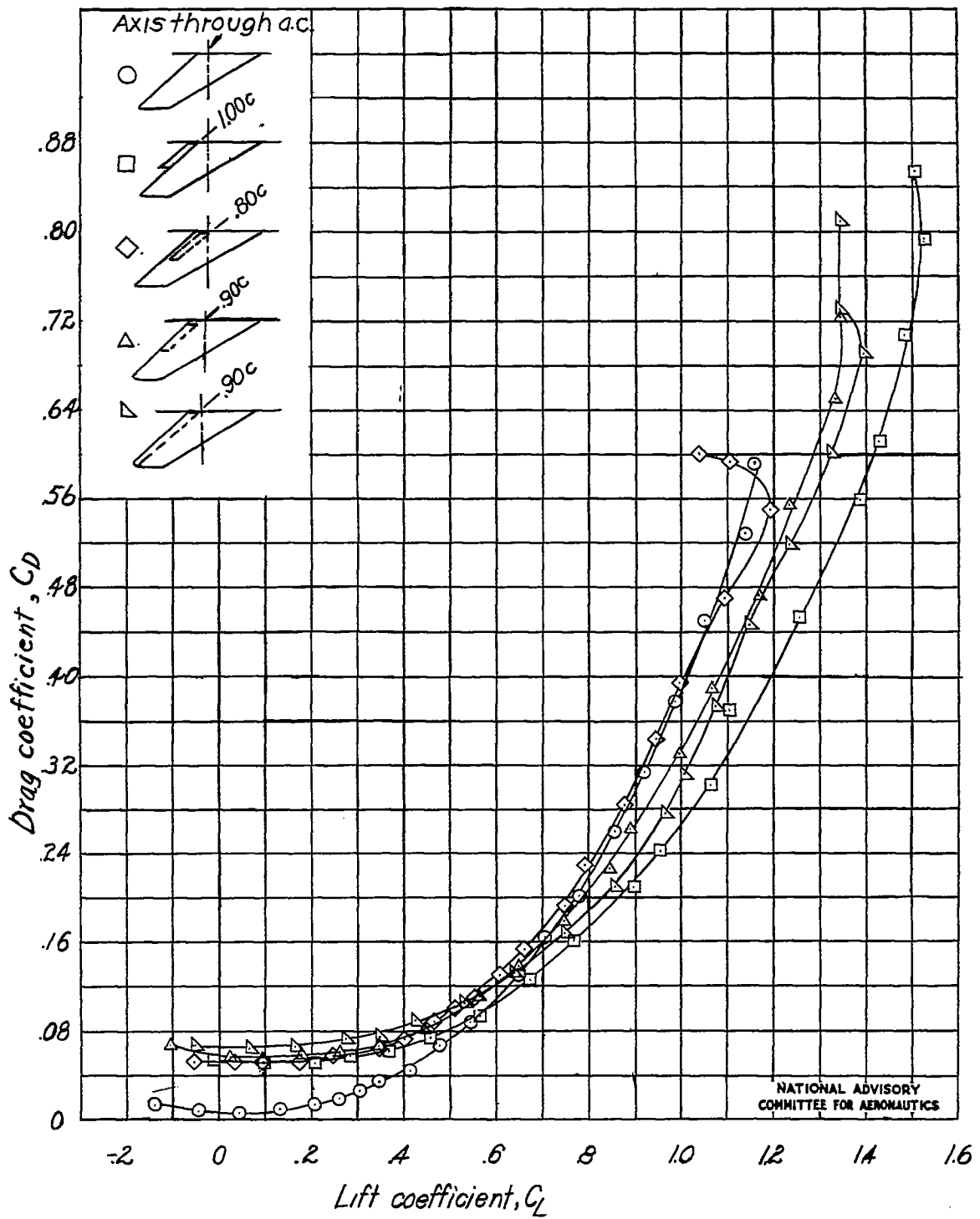


Figure 25.- Continued.

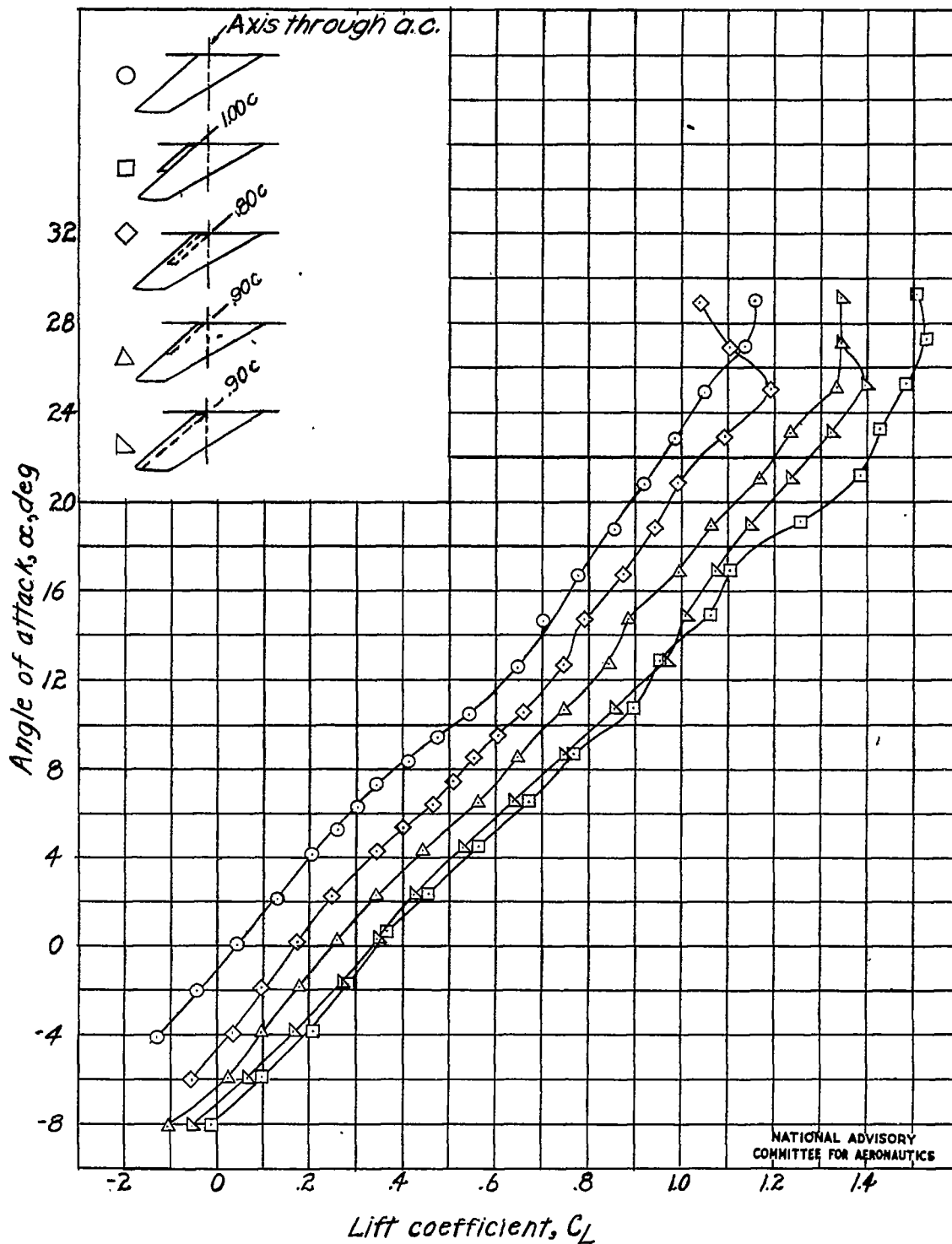


Figure 25.- Concluded.

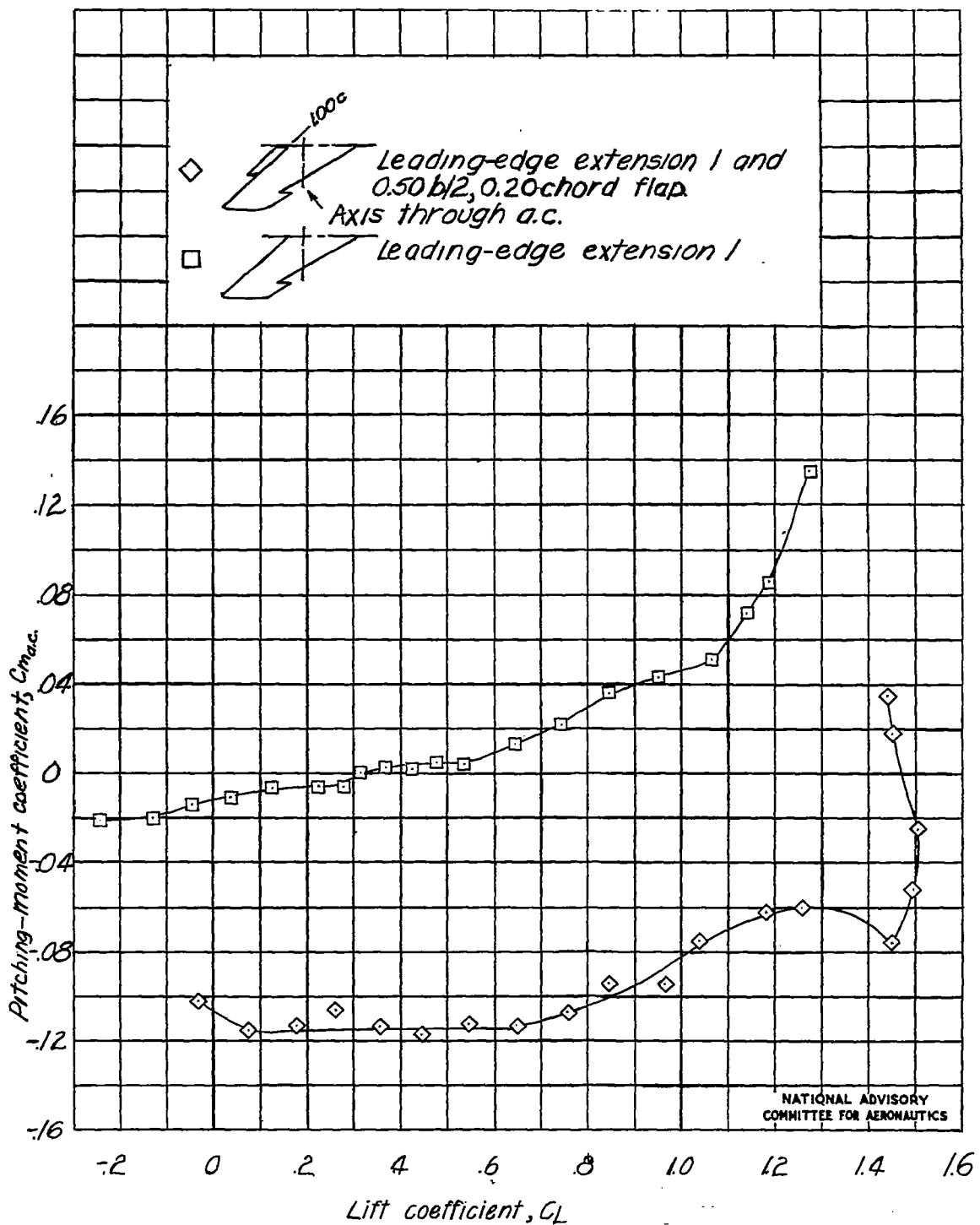


Figure 26.- Aerodynamic characteristics of 60° swept-back wing with leading-edge extension 1 with and without 0.50 b/2, 0.20-chord flap. Flap at $q = 10.1$ pounds per square foot, extension alone at $q = 20.1$ pounds per square foot.

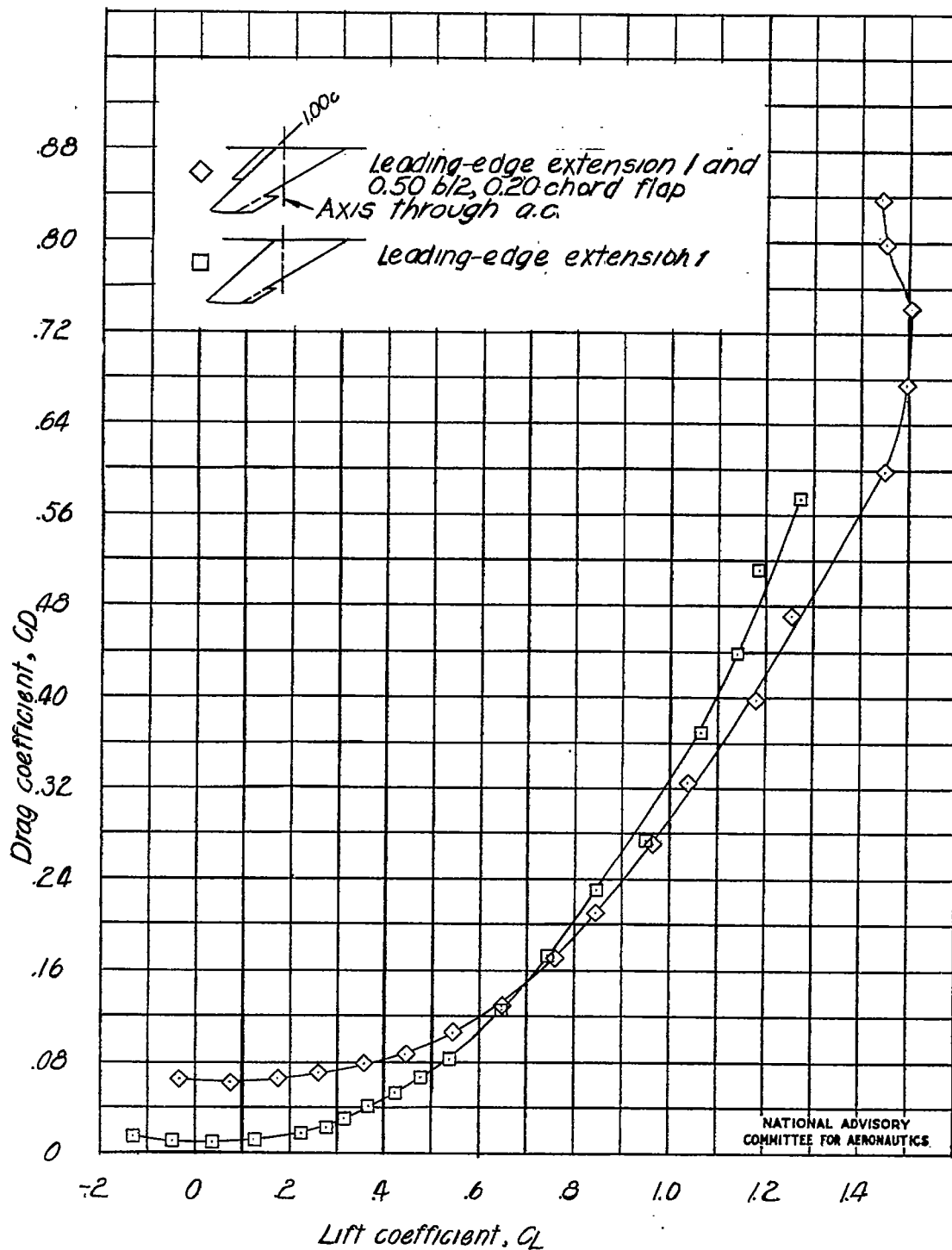


Figure 26.- Continued.

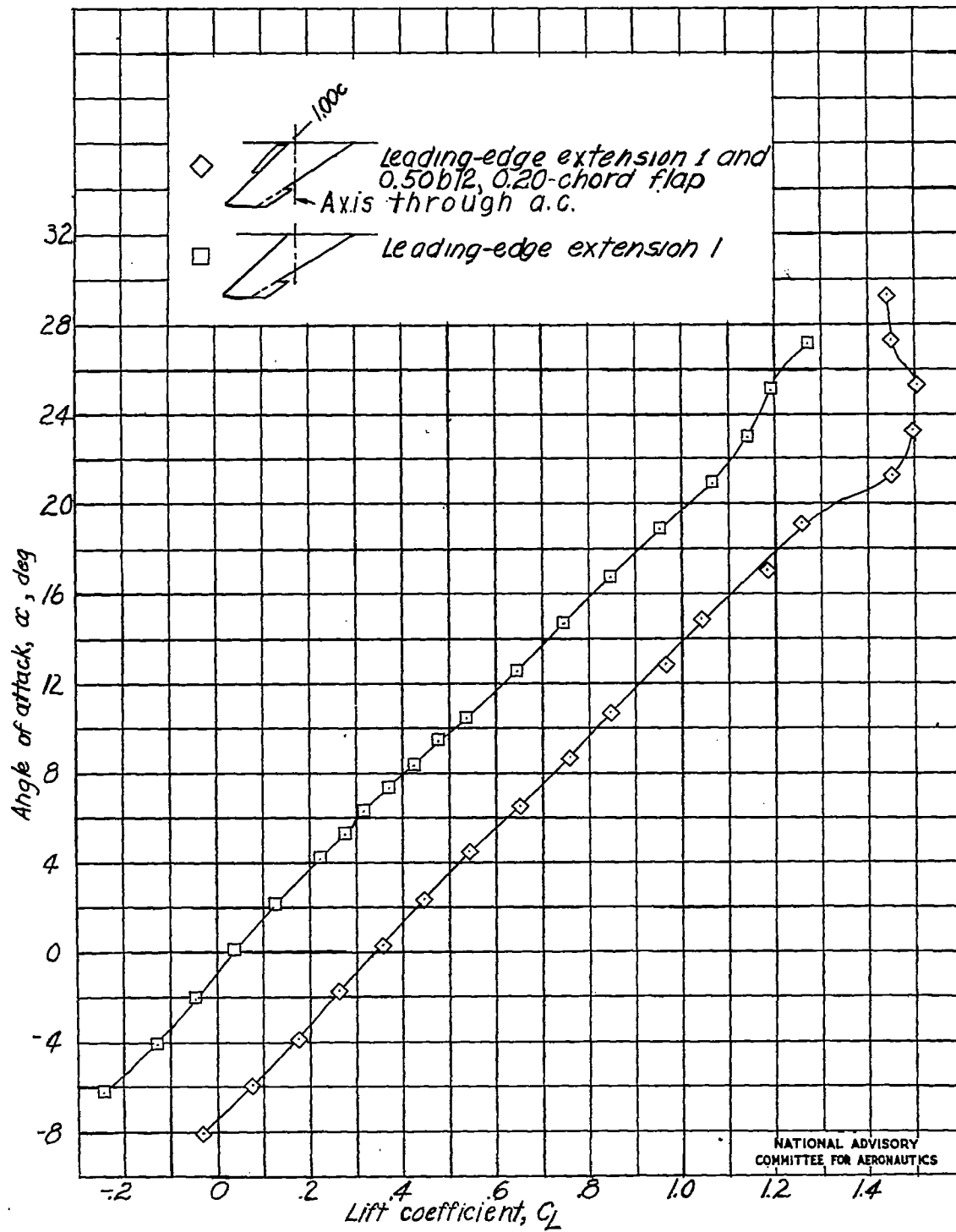


Figure 26.- Concluded.

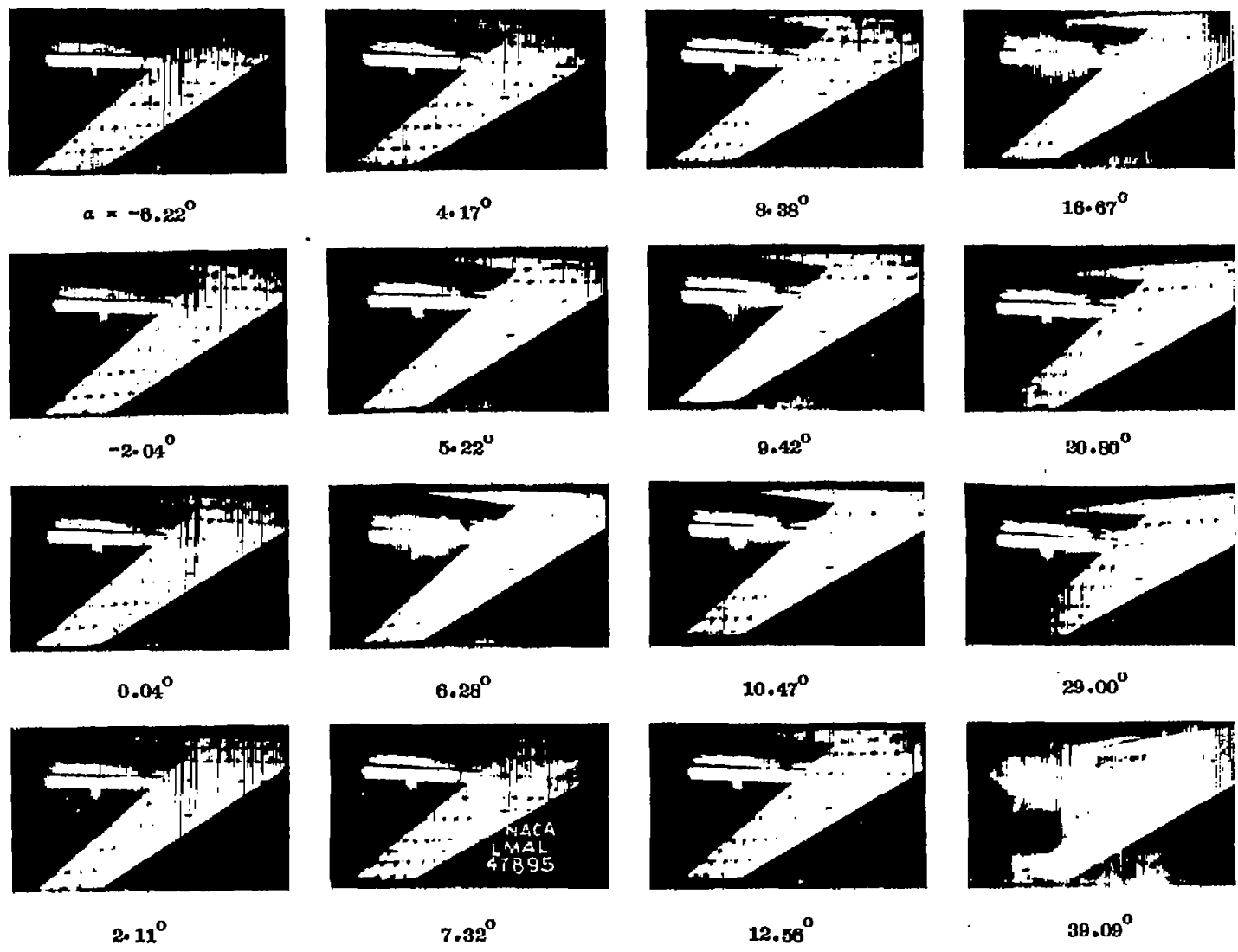


Figure 27.- Tuft study over upper surface of plain 60° swept-back wing.

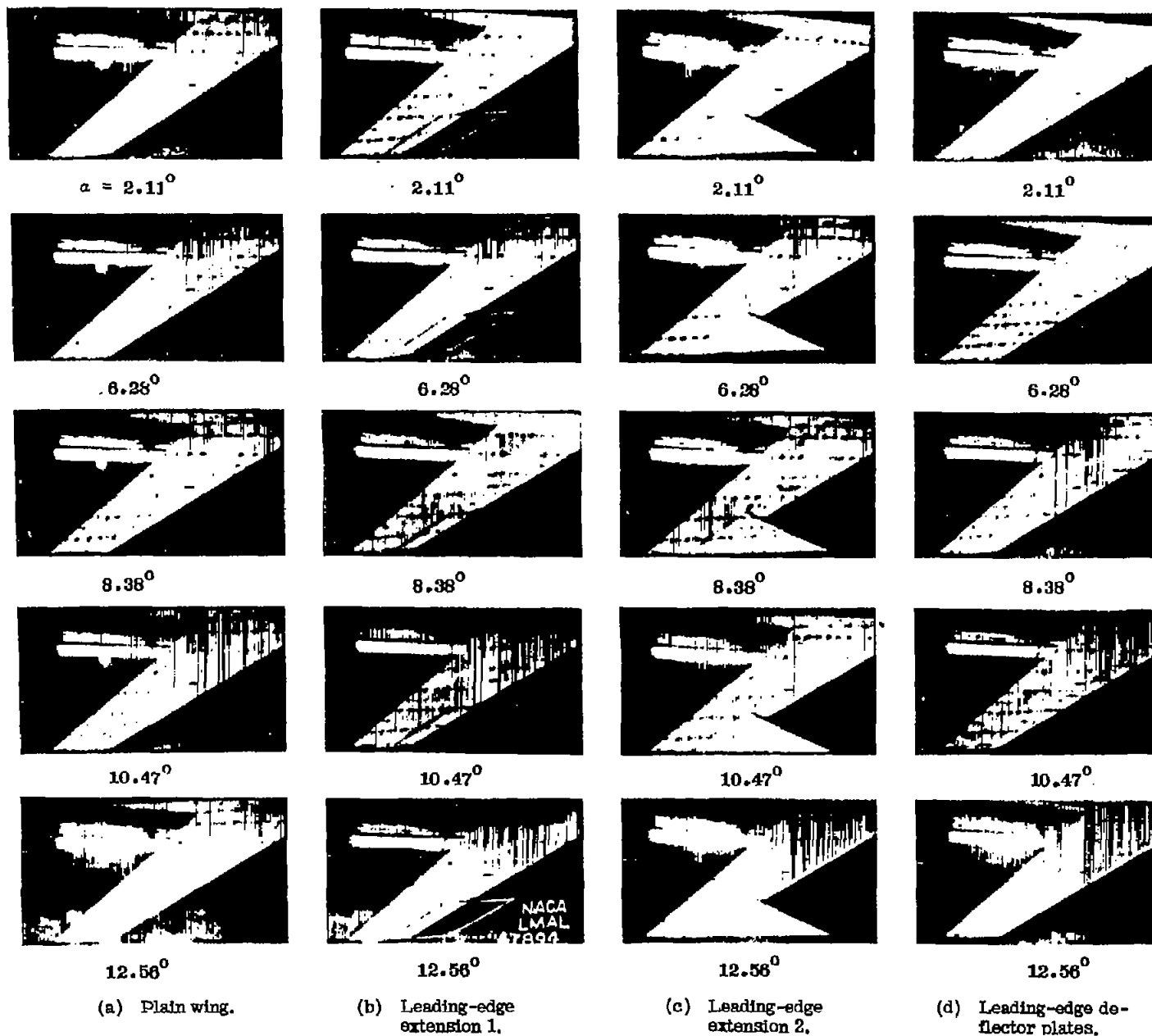
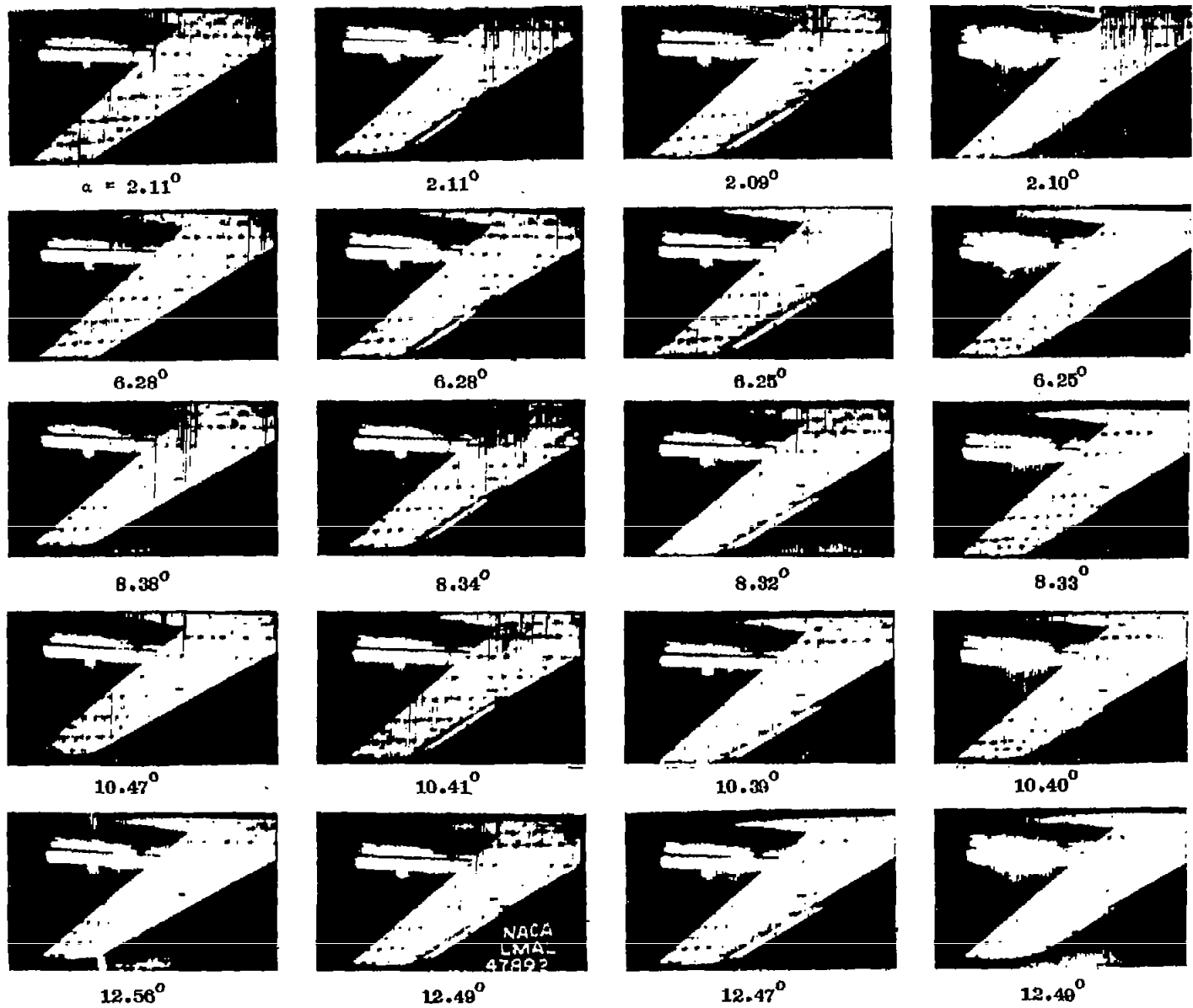


Figure 28.- Tuft studies over upper surface of 60° swept-back wing with leading-edge extensions and six deflector plates.



(a) Plain wing. (b) Slat 1. (c) Slat 2. (d) Leading-edge flap.

Figure 29.- Tuft studies over upper surface of 60° swept-back wing with slats and leading-edge flap.

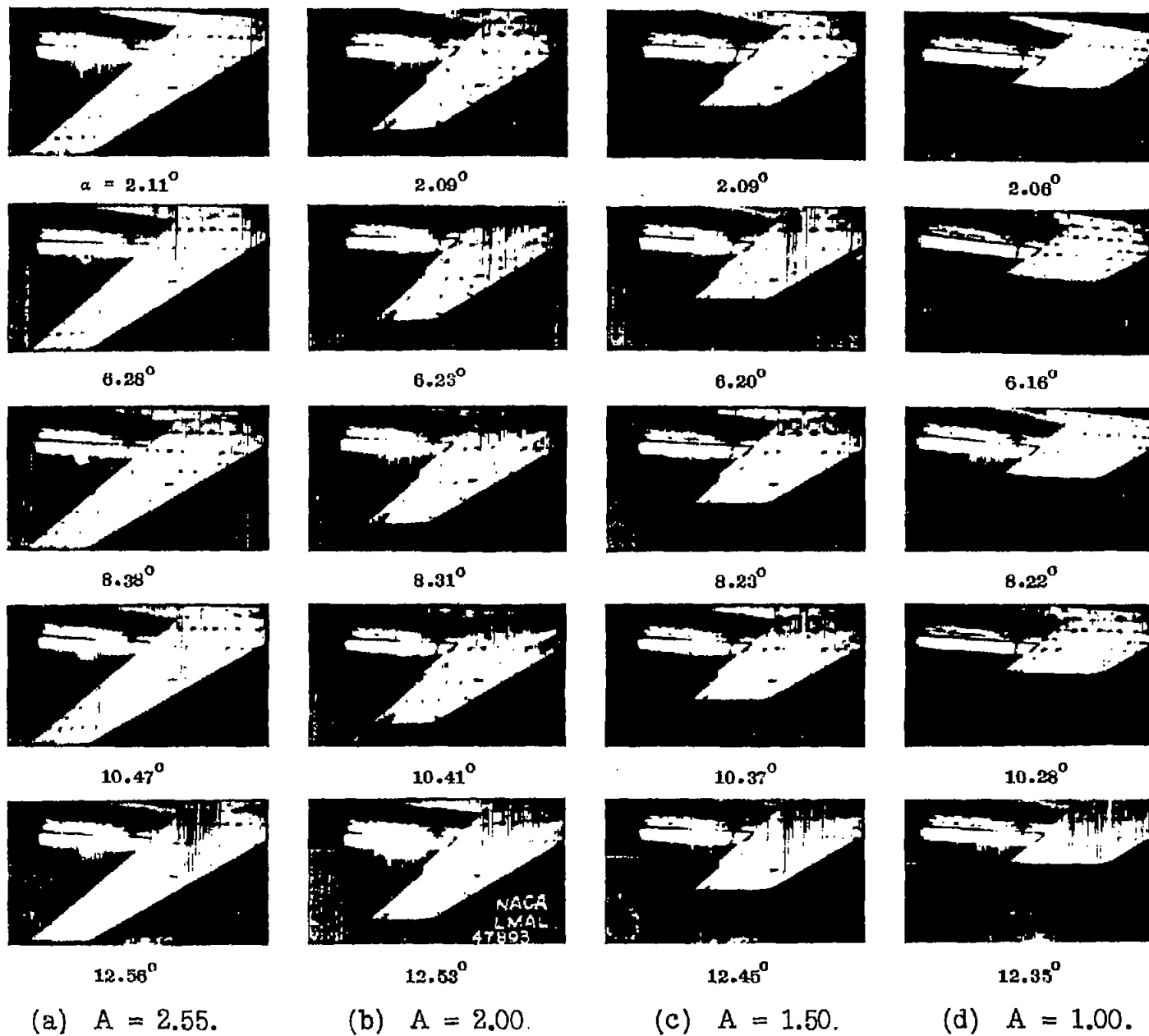


Figure 30.- Tuft studies over upper surface of 60° swept-back wings of various aspect ratios.